Doctoral Dissertation

Development of high performance photonic biopolyamides using 4,4'-diamino-α-truxillic acid

Yasuyoshi Funahashi

Supervisor: Tatsuo Kaneko

Graduate School of Advanced Science and Technology

Japan Advanced Institute of Science and Technology

[Materials Science]

March 2023

Abstract

Bioplastics have been the subject of much research in recent years in the interest of a sustainable society. Bioplastics are also expected to contribute to transparent materials, one of the most important applications of plastics. In order to apply bioplastics as transparent materials, in addition to high transparency, it is desirable for bioplastics to have mechanical, thermal, and moldability properties. In this study, the other focused on biopolyamides derived from 4-aminocinnamic acid as high-performance transparent bioplastics.

This thesis is composed of following five chapters: Chapter 1 describes the background and objectives of this research.

Chapter 2 describes the synthesis of *co*-polymers with aliphatic dicarboxylic acids and the preparation of tough fibers and self-standing thin membranes. The mechanical properties of biopolyamides were controlled by selecting the type and quantity ratio of 4-aminocinnamic acid-derived diamines and dicarboxylic acids and aliphatic dicarboxylic acids for the synthesis of *co*-polymers.

In Chapter 3 describes controlling the solubility of biopolyamides and their composites with cellulose nanofibers. The methyl esters in the side chains of biopolyamides were hydrolyzed by alkali to give the polyamides water solubility. Further insolubilization was achieved by doping divalent metal ions into the prepared films. The toughness of the water-soluble polyamide was improved by compositing it with cellulose nanofibers while maintaining its transparency.

In Chapter 4 describes the control of refractive index by compositing with metal oxides. Composite membranes were prepared by sol-gel reaction of titanium or zirconium alkoxides. The refractive index of the resulting membranes was measured, and an increase in the refractive index was observed as the amount of metal oxide increased.

Composite films of titanium dioxide and biopolyamide were also prepared. The obtained films were transparent and flexible. Further TEM observation showed that titanium dioxide particles of a few nm in size were uniformly dispersed in the film.

Chapter 5 summarizes the design of optical materials based on 4-aminocinnamic acid-based biopolyamides.

In this study, the auther focused on the main and side chain structures of biopolyamides. Since the structure of biopolyamides has many parts in common with other polymers, I believe that it can be expanded to design materials based on other polymers.

Keywords: Biobased polymers, Polyamide, Cinnamic acid, Cellulose nanofibers, Nanocomposites.

Acknowledgement

The study presented in this dissertation has been performed under the direction of Professor Tatsuo Kaneko, Japan Advanced Institute of Science and Technology (JAIST), from 2019 to 2023. The author would like to express his deepest gratitude to his supervisor Professor Tatsuo Kaneko for his supervision, valuable guidance, kind encouragement, and support during this work.

The author would like to extend his appreciation to the committee members of this dissertation: his second supervisor Professor Toshiaki Taniike, Professor Masayuki Yamaguchi, Professor Kazuaki Matsumura, at JAIST and Associate Professor Ryohei Ishige, from Tokyo Institute of Technology.

The author is deeply grateful to Assistant Professor Kenji Takada for his excellent guidance and kind encouragement. This work would never have performed without his great supporting.

The author thanks all of members of Kaneko laboratory. In addition, the author would like to give his special thanks to Yohei Yoshinaka for his contributions to this dissertation work.

In addition, the author would like to thank to Shoko Kobayashi, Tatsuya Murakami and Koichi Higashimine, technicians of Center for Nano Materials and Technology in JAIST for their assistance in sample observation and measurement.

Finally, the author would like to express his deep gratitude to his family for their understanding, support, and encouragement throughout his study in JAIST.

March 2023

Yasuyoshi Funahashi

Contents

Chapter 1. General introduction

1.1 Bioplastics

Plastic materials are applied in various fields due to their excellent moldability, lightness, and chemical stability. On the other hand, the social aspect of plastic, including its use and production, is changing due to its dependence on petroleum resources for the majority of its raw materials and the waste problems caused by the flow of plastic into the oceans.[1-3]

One strategy to address these issues is bioplastics.[4-8] Bioplastics are known as polymeric materials produced from natural or biological raw materials. Bioplastics include those that use bio-derived molecules as monomers as raw materials for polymers and those that use high molecular weight materials such as starch, either as is or modified.

Known examples of the former include poly (lactic acid) (PLA)[9-12], polyamide 11 (PA11)[13-15], and bio-polyethylene (BPE)[16-18]. In addition to starch[19,20], cellulose acetate[21] and cellulose nanofibers (CNF)[22-25] are known as representative examples of the latter. Polymers produced by microorganisms such as polyhydroxyalkanoic acid (PHA) have also been studied as bioplastics.[26,27]

Bioplastics are known to be degradable in the environment, including biodegradable, and less degradable and more durable.

Degradable plastics are expected to make a strong contribution to the waste problems if they are put into practical use.

On the other hand, even poorly degradable plastics can contribute to environmental problems in that they do not use petroleum as a raw material and that they can reduce carbon dioxide in the atmosphere through long-term use of plastics made from raw materials produced by carbon fixation by plants and other substances.

Against this background, the production of bioplastics has been increasing and is expected to continue to do so in the future. Therefore, it is important to develop bioplastics with higher performance or functionality (Figure 1-1).

Figure 1-1. Global production capacities of bioplastics.[28]

1.2 Water-soluble polymers[29-38]

Most commonly used plastic materials are hydrophobic, such as polyethylene (PE) and polypropylene (PP), and do not exhibit water solubility. Most commonly used plastic materials are hydrophobic, such as polyethylene and polypropylene, and do not exhibit water solubility. This is because water is a common molecule in the environment, and water solubility and hydrophilicity reduce the durability of materials.

On the other hand, many water-soluble or hydrophilic polymers are also known, whether synthetic or natural. In nature, water makes up the majority of the bodies of most living organisms, so many biopolymers are also hydrophilic. Synthetic polymers have also been developed that are designed to be water-soluble and hydrophilic for in vivo use. In addition, by adding water solubility to polymers, it is expected to enable clean molding process without using organic solvents, or to develop into hydrogels.

Especially for engineering plastics, which are difficult to thermoform, water solubility is an important material design policy.

1.3 Photonics materials

Transparency and other optical properties are very important functions for material science.

Transparent materials are applied in a very wide range of fields. In particular, transparent polymer materials are used in various applications such as food packaging[39], containers[40,41], coatings[42], windows, and lenses[43,44] due to their flexibility and processability.

Especially in recent years, the application of polymer materials in fields such as electronics is expected to grow. To achieve this, polymer materials must not only have transparency, but also heat resistance and mechanical properties that can withstand high-temperature processes such as sputtering. In addition, it is important to control optical properties other than transparency, such as refractive index. However, many transparent polymers have low heat resistance, and it is not easy to control the refractive index, especially to achieve a high refractive index.[45-47]

1.4 4-aminocinnamic acid-based polyamide[48-50]

In this study, I focused on 4-aminocinnamic acid-based polyamide as high-performance transparent polymer materials (Figure 1-2). 4-aminocinnamic acid is a bio-derived molecule that is naturally occurring and can be produced by genetically modified Escherichia coli.

This polyamide has a cyclobutane structure in the main chain, which acts to break the π-electron conjugation between adjacent conjugated rings in the molecule, and has

bulky benzene rings in both the main and side chains, which gives it excellent mechanical and thermal properties as well as high transparency. It also has a low birefringence index because the electron density in both the parallel and perpendicular directions to the main frame does not vary considerably.

I have considered the possibility of synthesizing a higher-performance polymer from this polyamide by using a third monomer in addition to the two 4-aminocinnamic acid-derived monomers as a base for the *co*-polyamide. In addition, I thought that water solubility could be added by hydrolyzing the methyl esters of the side chains to form metal salts. Furthermore, by controlling the solubility, I thought that it would be possible to combine not only with hydrophobic fillers but also with hydrophilic fillers such as cellulose nanofibers and fine particles such as titanium dioxide.

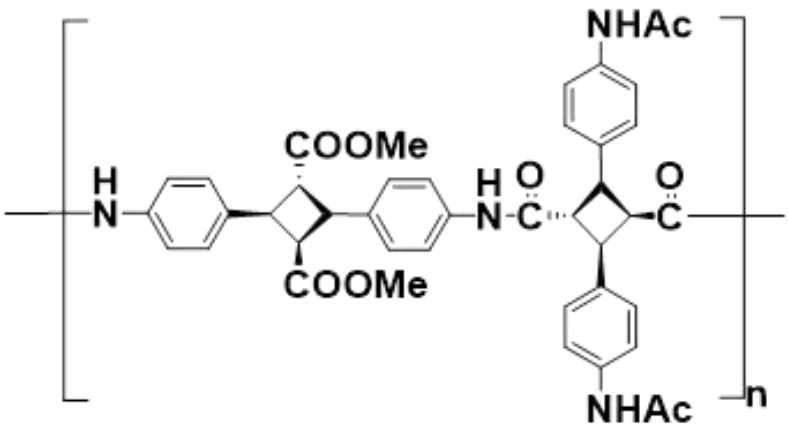

Figure 1-2. Structure of 4-aminocinnamic acid-based polyamide.

1.5 Research purposes

The objective of this research is to develop high-performance organic glass nanohybrid materials by synthesizing *co*-polyamides based on 4-aminocinnamic acid-derived polyamides, creating nanocomposites by introducing metal ions, hybridizing them by mixing them with fillers, and evaluating their physical properties.

REFERENCES

1. Pabortsava, K.; Lampitt, R., S., High concentrations of plastic hidden beneath the surface of the Atlantic Ocean, NATURE COMMUNICATIONS, **2020**, *11*, 4073.
2. Jambeck, J., R.; Geyer, R.; Wilcox,C.; Siegler, T.,R.; Perryman, M.; Andrady, A.; Narayan, R.; Law, K., L., Plastic waste inputs from land into the ocean, *Science*, **2015**, *347*, 768 – 771.
3. Cózara, A.; Echevarría, F.; González-Gordillo, J. J.; Irigoien, X.; Úbeda, B.; Hernández-León, M. L. S.; Palma, A. T.; Navarro, S.; García-de-Lomas, J.; Ruizg, A.; Fernández-de-Puelles, Duarte., C. M., Plastic debris in the open ocean, *PNAS*, **2014**., *111*, 10239–10244.
4. Manavitehrani, I.; Fathi, A.; Badr,H.; Daly, S.; Shirazi, A. N.; Dehghani, F., Biomedical Applications of Biodegradable Polyesters, *Polymers* **2016**, *8*, 20.

5. Haider, T. P.; Völker, C.; Kramm, J.; Landfester,K.; Wurm, F. R., Plastics of the Future? The Impact of Biodegradable Polymers on the Environment and on Society, *Angew.Chem.Int.Ed*.**2019**,*58*,50–62.

6. Kale, G.; Kijchavengkul,T.; Auras, R.; Rubino, M:; Selke, S. E.; Singh, S. P.,Compostability of Bioplastic Packaging Materials: An Overview, *Macromol. Biosci.* **2007**,*7*,255–27

7. Bilo,F.; Pandini, S.; Sartore, L.; Depero, L., E.; Gargiulo, G.; Bonassi A.; Federici, S.; Bontempi, E., A sustainable bioplastic obtained from rice straw, *Journal of Cleaner Production*, **2018** ,*200*, 357e36.

8. Jariyasakoolroj, P.; Leelaphiwat, P.; Harnkarnsujarit, N.; Advances in research and development ofbioplastic for food packaging, *J Sci Food Agric*, **2020**,*100*, 5032–504.

9. Okamura, Y.; Kabata, K.; Kinoshita, M.; Saitoh, D.; Takeoka, S., Free-Standing Biodegradable Poly(lactic acid) Nanosheet for Sealing Operations in Surgery. *Advanced Materials* **2009,** *21* (43), 4388-4392.

10. Fujino, K.; Kinoshita, M.; Saitoh, A.; Yano, H.; Nishikawa, K.; Fujie, T.; Iwaya, K.; Kakihara, M.; Takeoka, S.; Saitoh, D.; Tanaka, Y., Novel technique of overlaying a poly-l-lactic acid nanosheet for adhesion prophylaxis and fixation of intraperitoneal onlay polypropylene mesh in a rabbit model. *Surgical Endoscopy* **2011,** *25* (10), 3428.

11. Miyazaki, H.; Kinoshita, M.; Saito, A.; Fujie, T.; Kabata, K.; Hara, E.; Ono, S.; Takeoka, S.; Saitoh, D., An ultrathin poly(L-lactic acid) nanosheet as a burn wound dressing for protection against bacterial infection. *Wound Repair Regen* **2012,** *20* (4), 573-9.

12. Pensabene, V.; Taccola, S.; Ricotti, L.; Ciofani, G.; Menciassi, A.; Perut, F.; Salerno, M.; Dario, P.; Baldini, N., Flexible polymeric ultrathin film for mesenchymal stem cell differentiation. *Acta Biomaterialia* **2011,** *7* (7), 2883-2891.

13. Martino, L.; Basilissi, L.; Farina, H.; Ortenzi, M. A.; Zini, E.; Silvestro, G. D; Scandola, M, Bio-based polyamide 11: Synthesis, rheology and solid-state properties of star structures, *European Polymer Journal* **2014**, *59*, 69-77.

14. Oliver-Ortega, H.; Granda L.A.; Espinach, F.X.; Mendez, J.A.; Julian, F.; Mutje, P.; Tensile properties and micromechanical analysis of stone groundwood from softwood reinforced bio-based polyamide11 composites, *Composites Science and Technology* **2016**,*132* 123-130.

15. Nanni, A.; Messori, M., Thermo-mechanical properties and creep modelling of wine lees filled Polyamide 11 (PA11) and Polybutylene succinate (PBS) bio-composites, *Composites Science and Technology*, **2020**, *188*, 107974.

16. Siracusa, V.; Blanco, I.; Bio-Polyethylene (Bio-PE), Bio-Polypropylene (Bio-PP) and Bio-Poly(ethylene terephthalate) (Bio-PET): Recent Developments in Bio-Based

Polymers Analogous to Petroleum-Derived Ones for Packaging and Engineering Applications, *Polymers* **2020**, *12*, 1641.

17. Mendieta, C. M.; Vallejos, M. E.; Felissia, F. E.; Chinga-Carrasco, G.; Area, M. C., Review: Bio-polyethylene from Wood Wastes, *Journal of Polymers and the Environment* **2020**, *28*,1–16.
18. Tarrés, Q.; Ardanuy, M., Evolution of Interfacial Shear Strength and Mean Intrinsic Single Strength in Biobased Composites from Bio-Polyethylene and Thermo-Mechanical Pulp-Corn Stover Fibers, *Polymers*, **2020**, *12*, 1308.
19. Gonzalez-Gutierrez, J.; Partal, P.; Garcia-Morales, M.; Gallegos, C., Development of highly-transparent protein/starch-based bioplastics, *Bioresource Technology*, **2010**, *101*, 2007–2013.
20. Rahma Anugrahwidya, R.;·Armynah, B.; Tahir, D., Bioplastics Starch-Based with Additional Fiber and Nanoparticle: Characteristics and Biodegradation Performance: A Review, *Journal of Polymers and the Environment*, **2021**, *29*, 3459–3476.
21. Melo, P. G.; Borges, M. F.; Ferreira, J. A.; Silva, M. V. B.; Ruggiero, R., Bio-Based Cellulose Acetate Films Reinforced with Lignin and Glycerol, *Int. J. Mol. Sci*., **2018**, *19*, 1143.

22. Saito, T.; Kimura, S.; Nishiyama, Y.; Isogai, A., Cellulose Nanofibers Prepared by TEMPO-Mediated Oxidation of Native Cellulose *Biomacromolecules*, **2007**, *8*, 2485-2491.

23. Isogai, A.; Saito, T.; Fukuzumi, H., TEMPO-oxidized cellulose nanofibers *Nanoscale*, **2011**, *3*, 71-85

24. Noguchi, T.; Niihara, K.; Kurashima, A.; Iwamoto, R;, Miura, T.; Koyama., A.; Endo, M.; Marubayashi., H.; Kumagai., A.; Jinnai, H.; Isogai, A., Cellulose nanofiber-reinforced rubber composites prepared by TEMPO-functionalization and elastic kneading., *Compos. Sci. Technol.,* **2021,** *210*, 108815.

25. Kim, H.; Roy, S.; Rhim, J., Effects of various types of cellulose nanofibers on the physical properties of the CNF-based films *J. Environ. Chem. Eng.*, **2021**, *9*,106043.

26. Jendrossek, D.; Schirmer, A.;·Schlegel, H. G., Biodegradation of polyhydroxyalkanoic acids, *Appl Microbiol Biotechnol* , **1996**, *46*, 451–463.

27. Odeniyi, O. A.; Adeola, O. J., Production and characterization of polyhydroxyalkanoic acid from Bacillus thuringiensis using different carbon substrates, *International Journal of Biological Macromolecules*, **2017** *104*, 407–413.

28. *World plastics production 2020, Plastics Europe, 2021. https://www.european-bioplastics.org/market/*

29. Katayose, S.; Kataoka, K.; Water-Soluble Polyion Complex Associates of DNA and

30. Poly(ethylene glycol)-Poly(L-lysine) Block Copolymer, *Bioconjugate Chem*. **1997**, *8*, 702−707.

31. Chen, J.; Spear, S. K.; Huddleston, J. G.; Rogers., R. D., Polyethylene glycol and solutions of polyethylene glycol as green reaction media, *Green Chem*., **2005**, *7*, 64-82.

32. Hua, F.; Qian. M., Synthesis of self-crosslinking sodium polyacrylate hydrogel and water-absorbing mechanism, *Journal of Materials Science*, **2001**,36, 731–738.

33. Liu, M.; Guo, T., Preparation and swelling properties of crosslinked sodium polyacrylate, *Applied Polymer Science*, **2001**, *82*,1515–1520.

34. Geesing, D.; Schmidhalter, U., Influence of sodium polyacrylate on the water-holding capacity of three different soils and effects on growth of wheat, *Soil Use and Management*, **2004**, *20*,207-209.

35. Lu., J.; Wang, T.; Drzal, L. T., Preparation and properties of microfibrillated cellulose polyvinyl alcohol composite, *Composites Part A: Applied Science and Manufacturing,* **2008***, 39.,* 738-746.

36. Peng, X.; Zhang, Z., Improvement of paint adhesion of environmentally friendly paint film on wood surface by plasma treatment, *Progress in Organic Coatings*, **2019**, *134*, 255

37. Sun, Q.; Schork, F., J.; Deng, Y., Water-based polymer/clay nanocomposite suspension for improving water and moisture barrier in coating *Compos. Sci. Technol.*, **2007**, *67*, 1823-1829.

38. Jia, L.; Zhou, C.; Sun, W.; Xu, L.; Yan, D.; Li, Z.; Water-based conductive ink for highly efficient electromagnetic interference shielding coating, *Chem. Eng. J.*, **2020**, *384*, 123368.

39. Barlow, C.Y.; Morgan, D.C., Polymer film packaging for food: An environmental assessment, Resources, *Conservation and Recycling*, **2013**, *78*, 74-80.

40. Westerhoff, P.; Prapaipong, P.; Shock, E.; Hillaireau, A., Antimony leaching from polyethylene terephthalate (PET) plastic used for bottled drinking water, *Water Research*, **2008**, *42*, 551-556.

41. Spaseska, D.; Civkaroska, M., *Journal of the University of Chemical Technology and Metallurgy*, **2010**, *45*, *4*, 379-384.

42. Chen, C.; Dou, L.;, Zhu, R.; Chung, C., Song, T., Zheng, Y. B.;Hawks, S., Li, G.; Weiss,P. S.; Yang, Y., Visibly Transparent Polymer Solar Cells Produced by Solution Processing, *ACS Nano,***2012**, *6,* 7185–7190.

43. Fan, Y.; Ren, H.; Wu, H., witchable Fresnel lens using polymer-stabilized liquid crystals, *Optics Express **2003** ,11*, 3080-3086.

44. Rowe,N. A.; Biswas,S.; Lloyd, I.C.; Primary IOL implantation in children: a risk analysis of foldable acrylic v PMMA lens*es, Br J Ophthalmol* **2004**, *88*, 481–485.

45. Lee, L.; Chen, W.; High-Refractive-Index Thin Films Prepared from Trialkoxysilane-Capped Poly(methyl methacrylate)-Titania Materials, *Chem. Mater.* , **2001**, *13*, 1137-1142.

46. Imai, Y.; Terahara, A.; Hakuta, Y.; Matsui, K.; Hayashi, H.; Ueno, N., Transparent poly(bisphenol A carbonate)-based nanocomposites with high refractive index nanoparticles, *European Polymer Journal* **200**9, *45* 630.

47. Jintokua, H.; Ihara, H., The simplest method for fabrication of high refractive index polymer–metal oxide hybrids based on a soap-free process,*Chem. Commun*., **2014**, *50*, 10611—10614.

48. Phanthuwongpakdee, J.; Babel, S.; Dwivedi, S.; Takada, K.; Hirayama, T.; Kaneko, T., Anion-Scavenging Biopolyamides from Quaternized 4-Aminocinnamic Acid Photodimers. *ACS Sustainable Chemistry & Engineering* **2020,** *8* (9), 3786-3795.

49. Takada, K.; Mae, Y.; Kaneko, T., Fluorinated and Bio-Based Polyamides with High Transparencies and Low Yellowness Index. *Polymers (Basel)* **2018,** *10* (12).

50. Tateyama, S.; Masuo, S.; Suvannasara, P.; Oka, Y.; Miyazato, A.; Yasaki, K.; Teerawatananond, T.; Muangsin, N.; Zhou, S.; Kawasaki, Y.; Zhu, L.; Zhou, Z.; Takaya,

N.; Kaneko, T., Ultrastrong, Transparent Polytruxillamides Derived from Microbial Photodimers. *Macromolecules* **2016,** *49* (9), 3336-3342.

Chapter 2. Self-standing Nanomembranes of Super-Tough polyamides

2.1 Introduction and research background

Nanomembranes have been used as coating materials in architectural, electronic, and biomedical applications to protect substrates from external stimuli.[1-3] Nanomembrane refers to a quasi-2D structure with macroscopic surface area and thickness ranging from 10 to several hundred nanometers. The thickness ranges from 1 to 100 nm and the aspect ratio of size to thickness is greater than 10^6. [4] Such a high aspect ratio facilitates the handling of the nanomembrane; however, the self-standing property that allows the nanomembrane to be physically removed from the supporting substrate while maintaining mechanical properties results from the toughness of the resin. So far nanomembranes are developed using polymers such as poly(lactic acid), [5-8] poly(ethylene glycol), [9] poly(methyl acrylate)[10, 11], and their derivatives or composites[12]. However, all these resins have low heat resistance and exhibit certain drawbacks, when used as a base material for insulating substrates. Developing self-standing nanomembranes that exhibit flexibility and optical transparency using high-performance polymers would be an innovative development in the field of nanotechnology, including miniaturized devices. [13-15]

Some of the polymers that exhibit high heat resistance and mechanical strength include aromatic polyimide and polyamide. These polymers exhibit high performance owing to the interaction between the aromatic rings, various imide rings, and amide bonds. [16-19]

Despite having such high performance, most aromatic polymers have the disadvantage of low toughness owing to their high rigidity. Recently, biobased high-performance plastics were developed as super-strong optically transparent plastics of polyimides[20-26] and polyamides from an aromatic bio-produced resource, photodimer derivatives of 4-aminocinnamic acid (4ACA) [27-29], which is produced from genetically manipulated *Escherichia coli* to realize a sustainable society. [30-33] Specifically, the biobased polyamides showed higher thermal and mechanical stability compared to conventional organic glasses, such as poly(ethylene terephthalate)[34] , poly(methyl methacrylate),[35] polycarbonates,[36, 37] cycloolefin polymers,[38] and nanocellulose films.[39] However, in a previous study, only fibers could be obtained, and a method for fabricating high-strength films was not established.

In the present study, to obtain ultra-high toughness, various aliphatic dicarboxylic acids with different ratios were incorporated into 4ACA-based polyamides. Fabricated fibers and films show the high strain energy density (toughness) exceeding spider silk[40] and the mechanism of the high toughness was evaluated using *in situ* infrared and X-ray diffraction spectroscopy. The resulting spin-cast nanomembranes with a thickness around 200 nm are peeled off the substrate without breakage and self-standing.

2.2 Experimental

2.2.1 Materials

Dehydrated pyridine (moisture content: maximum 0.005 %) was purchased from Wako Pure Chemical Industries. Triphenyl phosphite was purchased from Junsei Chemical. Acetone, methanol, *n*-hexane, dehydrated *N*-methyl-2-pyrrolidone (NMP, moisture content: 0.005 %), and *N,N*-dimethylformamide (DMF) were purchased from Kanto Chemical. All the materials described above were used as received. Adipic acid (**C6**), pimelic acid (**C7**), suberic acid (**C8**), azelaic acid (**C9**) and sebacic acid (**C10**) were purchased from Tokyo Chemical Industry and recrystallized by acetone. 4,4'-diamino-*α*-truxillic acid dimethyl ester (**M1**) and 4,4'-diacetamido-*α*-truxillic acid (**M2**) were synthesized by presented literatures.

2.2.2 Syntheses of *co*-polyamides

4,4'-Diamino-*α*-truxillic acid dimethyl ester (**M1**) and 4,4'-diacetamido-*α*-truxillic acid (**M2**) were synthesized as previously described (Scheme 2-1). Polyamides were synthesized from **M1** and **M2**; *co*-polyamides were synthesized from **M1** and **M2** and an aliphatic dicarboxylic acid such as adipic acid (**C6**), pimeric acid (**C7**), suberic acid (**C8**), azelaic acid (**C9**), or sebacic acid (**C10**). Thus, a series of polyamides was obtained in quantitative yields.

One of the reaction procedures was follows. M1 (0.282 g, 0.796 mmol), M2 (0.245 g, 0.597 mmol), aliphatic dicarboxylic acid (0.199 mmol; adipic acid (C6, 29.1 mg); pimeric acid (C7, 31.8 mg); suberic acid (C8, 34.7 mg); azelaic acid (C9, 37.4 mg); sebacic acid (C10,

40.2 mg)), triphenyl phosphite (230 μL, 0.865 mmol), and pyridine (390 μL, 4.86 mmol) were added to *N*-methyl-2-pyrrolidone (800 μL) under N_2 atmosphere, and stirred for 24 hours at 80 °C. After the reactions, reaction mixture was diluted by DMF and the solution was reprecipitated to methanol for 2-times, after dry under vacuum at 150 °C to obtain the objective *co*-polyamide with quantitative yield (reaction condition of $[M1]_0/[M2]_0/[Cn]_0$, of 100/75/25).

Scheme 1. Syntheses of bio-based polyamides using 4,4'-diamino-*α*-truxillic acid dimethyl ester (M1), 4,4'-diacetamido-*α*-truxillic acid (M2), and various aliphatic dicarboxylic acids (C6–C10).

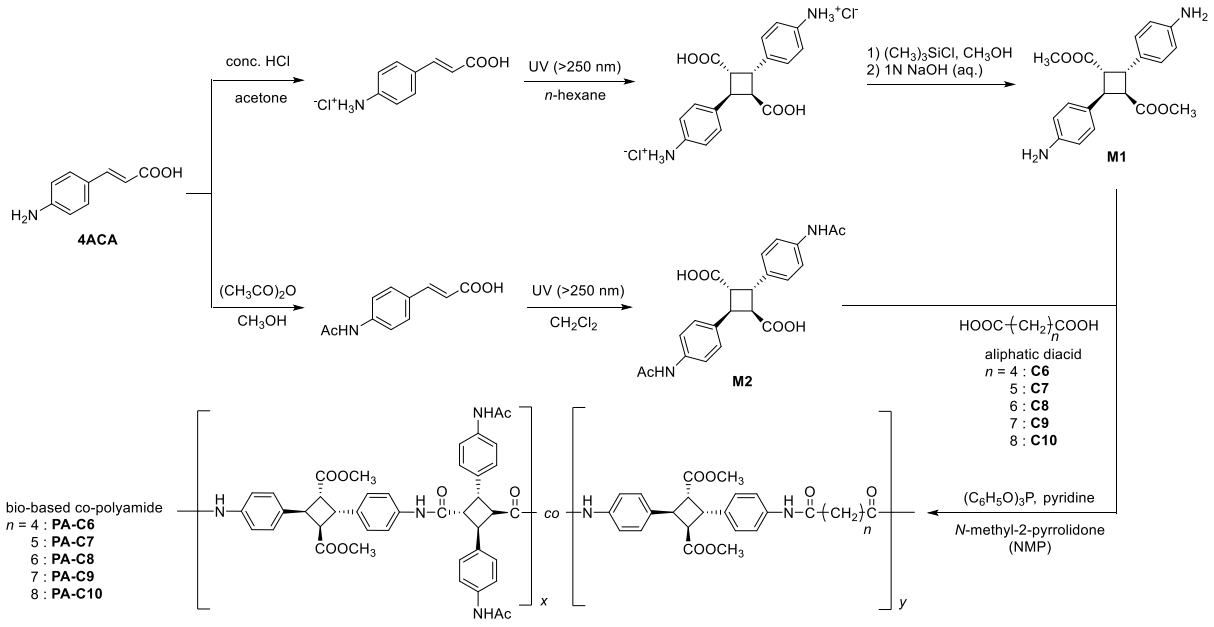

2.2.3 Preparation of fibers and nano membranes

Fibers

Fiber samples were prepared by wet spinning method for carried out tensile test. Some of the fibril were put on the glass plate and a few drops of DMF were added. The glass plate with *co*-polyamide and DMF solution was placed into the electric furnace whose temperature was around 230 °C. Solution was mixed by tweezers in the electric furnace and pulled up after it became viscous by DMF evaporation. Pulled up the viscous solution was kept as it was for 5 min to remove the DMF and fibers were prepared. (Figure 2-1A)

Membranes

The synthesized polyamides were dissolved into *N,N*-dimethylformamide (DMF) to obtain the solution with a concentration of 100 mg/ 3 mL, and the resulting 300 μL of solution was dropped on a glass plate (25 mm*25 mm, cleaned by ultrasonication for 1 hrs) fixed in a spin coating device（MIKASA, MS-A100）. Glass plates were rotated at a rotation speed of 1200 rpm for 60 sec. After the plate was transferred on a hot plate, the spin-cast membrane was dried at 150 °C for 1 hrs. The membranes were successfully peeled out of the glass substrate from membrane periphery by a paper-supported double side tape without breaking because of high toughness.

2.2.4 Characterization

Nuclear magnetic resonance (NMR) spectra (^{1}H at 400 MHz) were obtained by a

AVANCE III HD NMR spectrometer 400 MHz (BRUKER) using DMSO-d_6 as a solvent. Gel permeation chromatography (GPC) was performed on two of Shodex column (KD-805; range, 30k ~ 4,000k), column oven (GL Science, C0 631A, set as 40 °C), degassing unit (GL Science, DG 660B), pump (JASCO, PU-2080 Plus), refractive index detector (JASCO, 830-RI), ultraviolet detector (JASCO, UV-2075 plus) using 0.01 mol L^{-1} of LiBr solution of DMF as an eluent (flow rate, 1 mL min^{-1}). Thermal gravimetrical analysis (TGA) was carried out by STA 7200 (HITACHI) under nitrogen flow (flow rate, 200mL min^{-1}) from 25 °C to 800 °C at heating rate of 5 °C min^{-1}. Differential scanning calorimeter (DSC) was performed by SEIKO X-DSC7000T to measured glass transition temperature (T_g) which were measured from 25 °C to 300 °C at a heating rate of 10 °C min^{-1} (hold 5 min) with 5 mg sample. Mechanical strength was measured by using a tensile testing machine (Series 3360 Load Frame, Instron) with 0.50 mm min^{-1} as tension rate. Ultraviolet-Visible Absorption Spectroscopy (UV-Vis) was performed by V-670 (JASCO) in 200 nm to 800 nm as measured range. Fourier transform infrared spectroscopy (FT-IR) measurement was carried out using Spectrum 100 and Spectrum Spotlight 200 (Perkin Elmer) by transmission method. X-ray diffraction (XRD) measurements was performed by using Smart Lab (Rigaku) in wide angle X-ray diffraction (WAXD) as measurement mode with 180 second exposed time. Refractive indexes and thickness of nano-membranes which were adhered on glass plates were measured by using

an optical thickness meter (Otsuka Electronics).

2.2.5 *In situ* measurements

In situ measurement were carried out by FT-IR and XRD to trace the structural transitions of *co*-polyamide molecules through the tensile tests.[43] Fibers of PA-C10 with $[M1]_0/[M2]_0/[C10]_0$ of 100/25/75 were prepared for these measurements. Using a tool that could pull the fiber manually the fiber was stretched to keep each elongation at 10 to 100 % (Figure 2-1B), defined the elongation as follows: 100× (elongated fiber length – original fiber length)/original fiber length. Then, XRD and IR were measured while stress was applied to the fiber. IR measurements were made using fibers the thicknesses were less than 20 μm. XRD measurements were using 5 fibers for one sample.

Hermans' orientation function, *f*, was calculated to analyze the quantitative orientation behavior. Before calculating the function, the average orientation for a set of *hkl*, $\langle\cos^2\phi\rangle_{hkl}$, was calculated using the following equation:

$$\langle \cos^2\phi \rangle_{hkl} = \frac{\int_0^{\pi/2} I(\phi) \cos^2\phi \sin^2\phi \, d\phi}{\int_0^{\pi/2} I(\phi) \sin\phi \, d\phi} \qquad (1)$$

where ϕ is the azimuthal angle and $I(\phi)$ is the scattered intensity along the angle ϕ. From this average orientation $\langle\cos^2\phi\rangle_{hkl}$, Hermans' orientation function, *f*, was calculated using the

following equation:

$$f = \frac{3\langle cos^2\phi \rangle_{hkl} - 1}{2} \qquad (2)$$

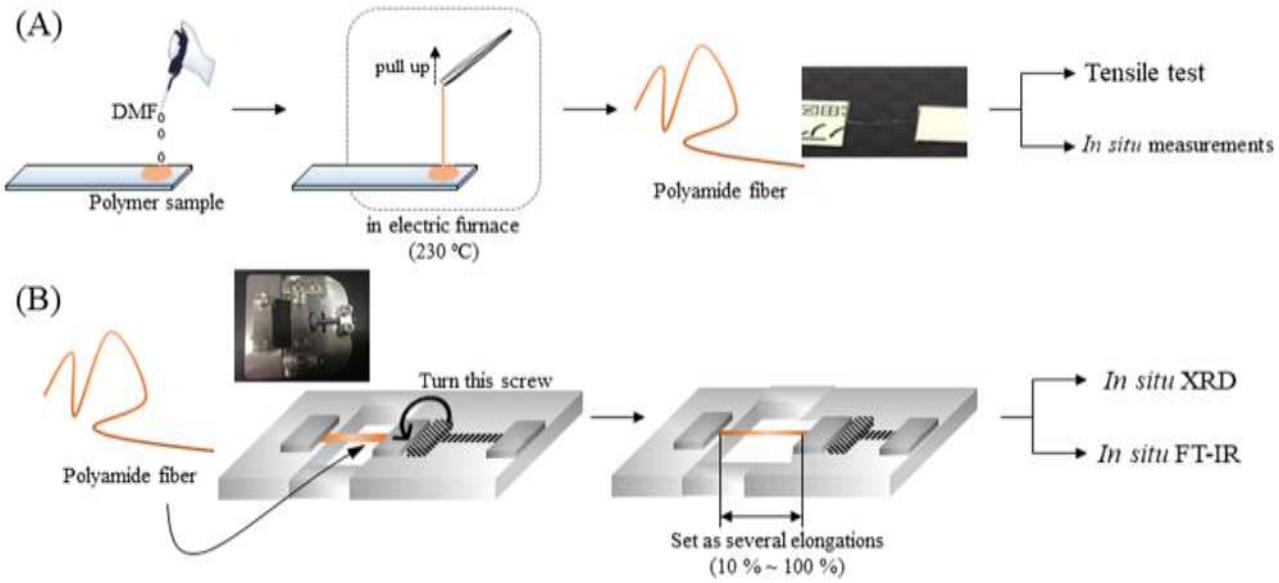

Figure 2-1. (A) Polyamide-fiber spinning process for tensile test and *in situ* measurements and (B) methodology of the *in situ* XRD and FT-IR measurements.

2.3 Results and discussion

The structural optimization of biopolyamides with diphenylcyclobutane behaving as a molecular spring was performed by changing the composition of aliphatic chains with different methylene numbers (*n* = 4, 5, 6, 7, 8) to prepare transparent and high-toughness polymers. All the polyamides were synthesized using bio-based aromatic monomers, M1 and M2, and aliphatic dicarboxylic acids (Cn) in the presence of a condensation reagent of pyridine and triphenylphosphine oxide. The obtained polyamides were purified by

reprecipitation in methanol to produce white fibrils.

^{1}H NMR spectra of biopolyamides were shown in figure 2-2,3,4,5, and 6. Structure and copolymerization ratios were confirmed by these spectra. The copolymerization ratios were corresponded closely to charge ratios of monomers.

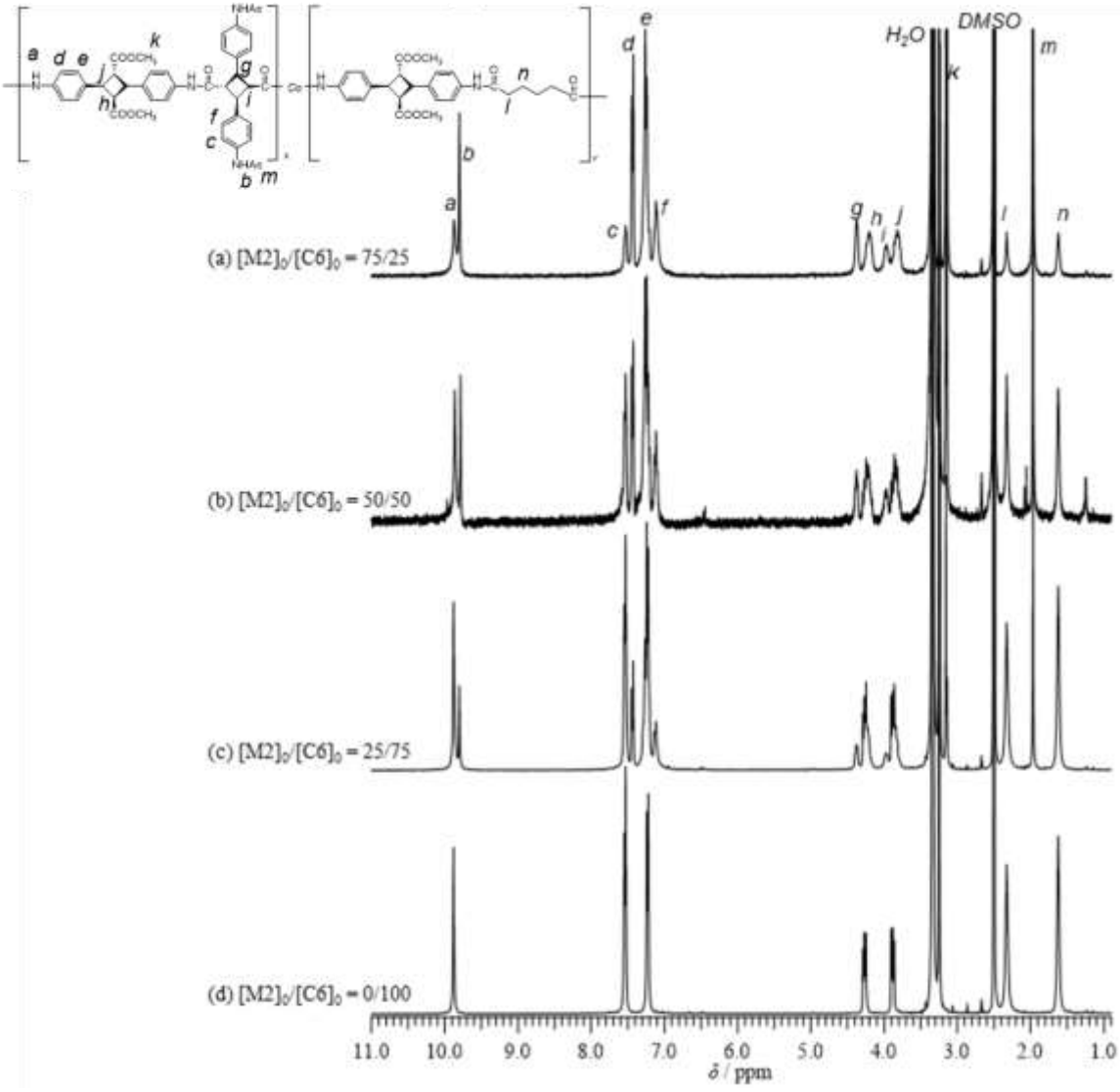

Figure 2-2. ^{1}H NMR spectra of PA-C6 with various monomer ratios $[M2]_0/[C6]_0$ (400MHz NMR; solvent, DMSO-d_6).

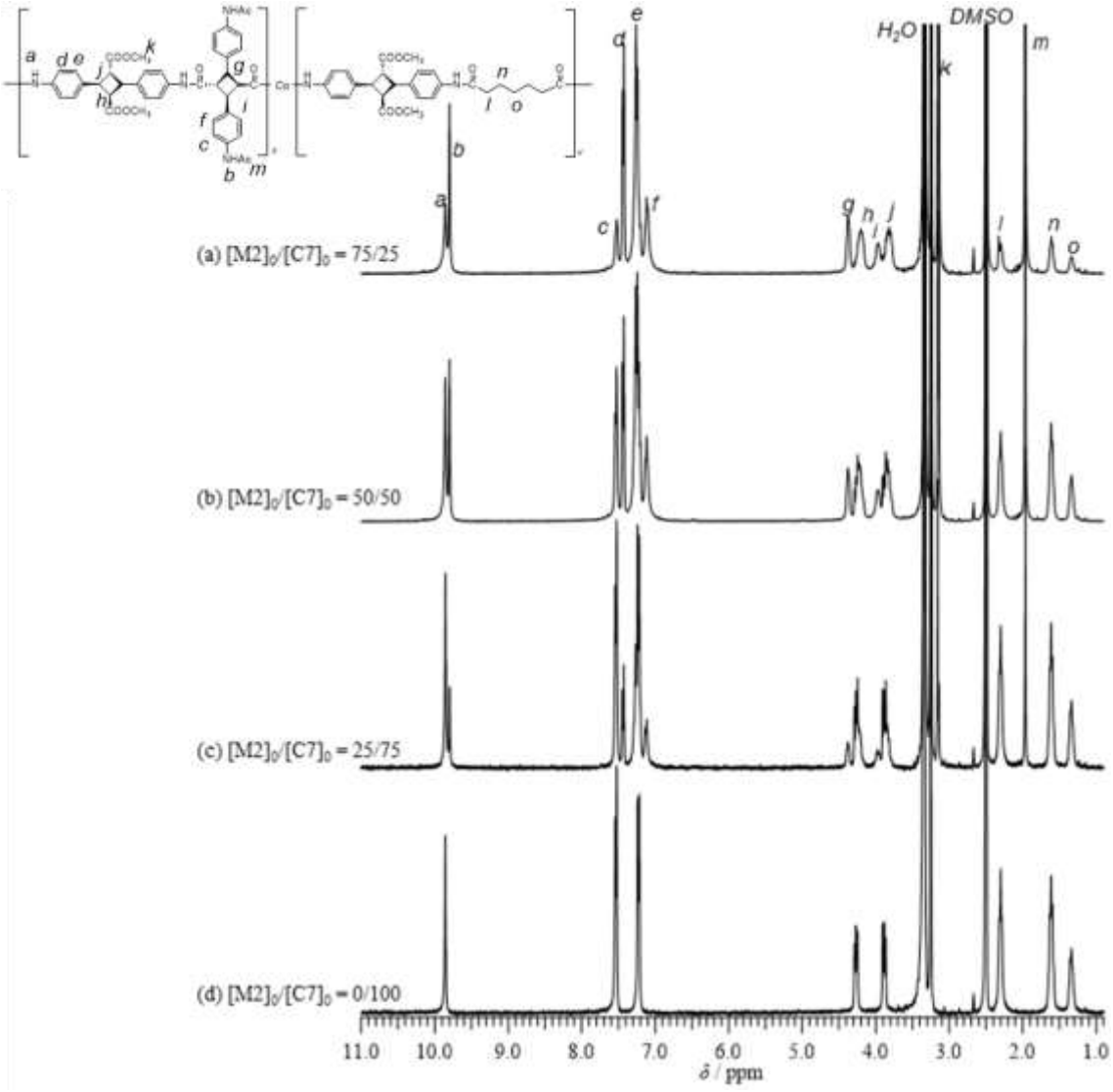

Figure 2-3. ^{1}H NMR spectra of PA-C7 with various monomer ratios $[M2]_0/[C7]_0$ (400MHz NMR; solvent, DMSO-d_6).

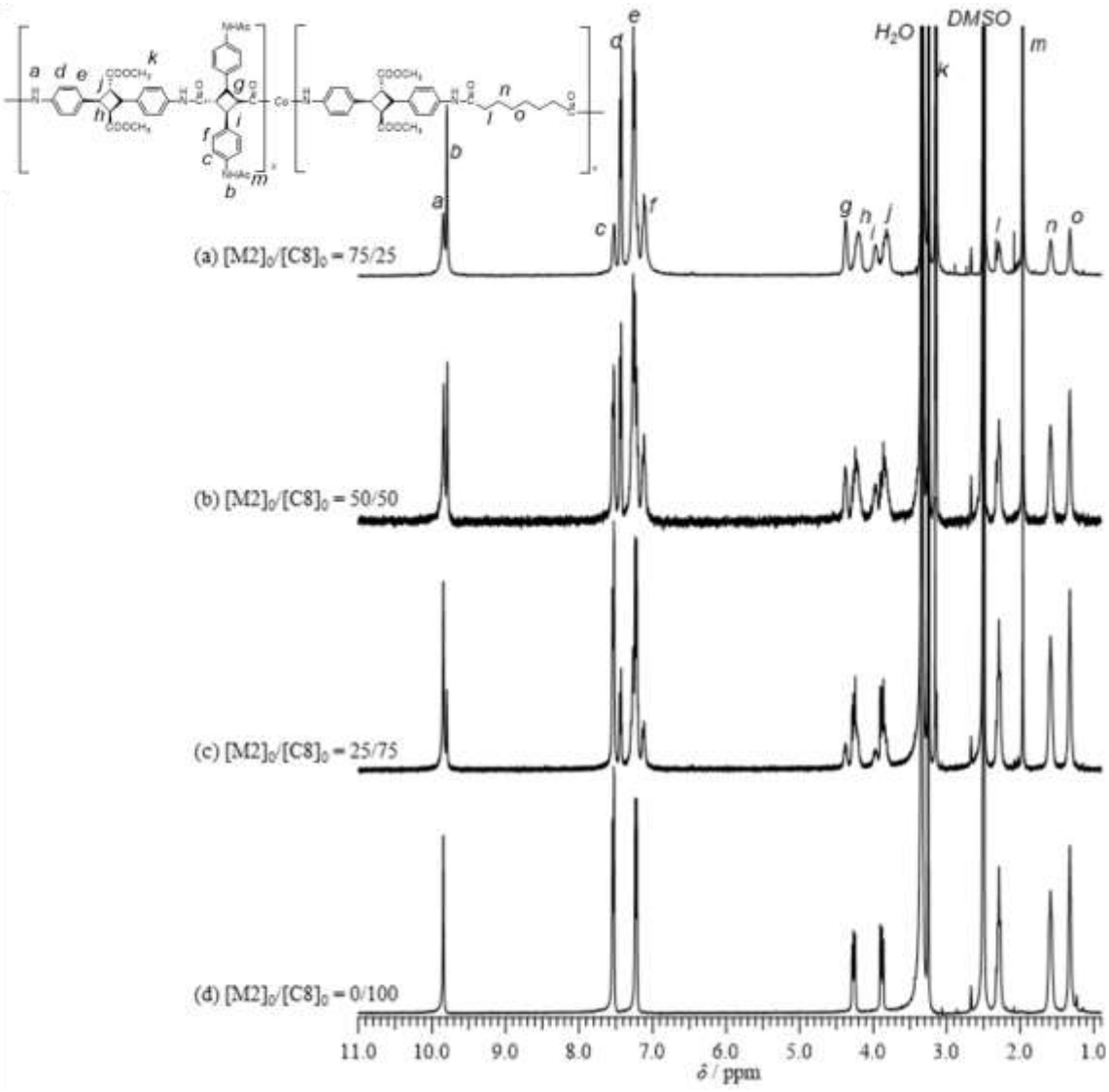

Figure 2-4. ^{1}H NMR spectra of PA-C8 with various monomer ratios $[M2]_0/[C8]_0$ (400MHz NMR; solvent, DMSO-d_6).

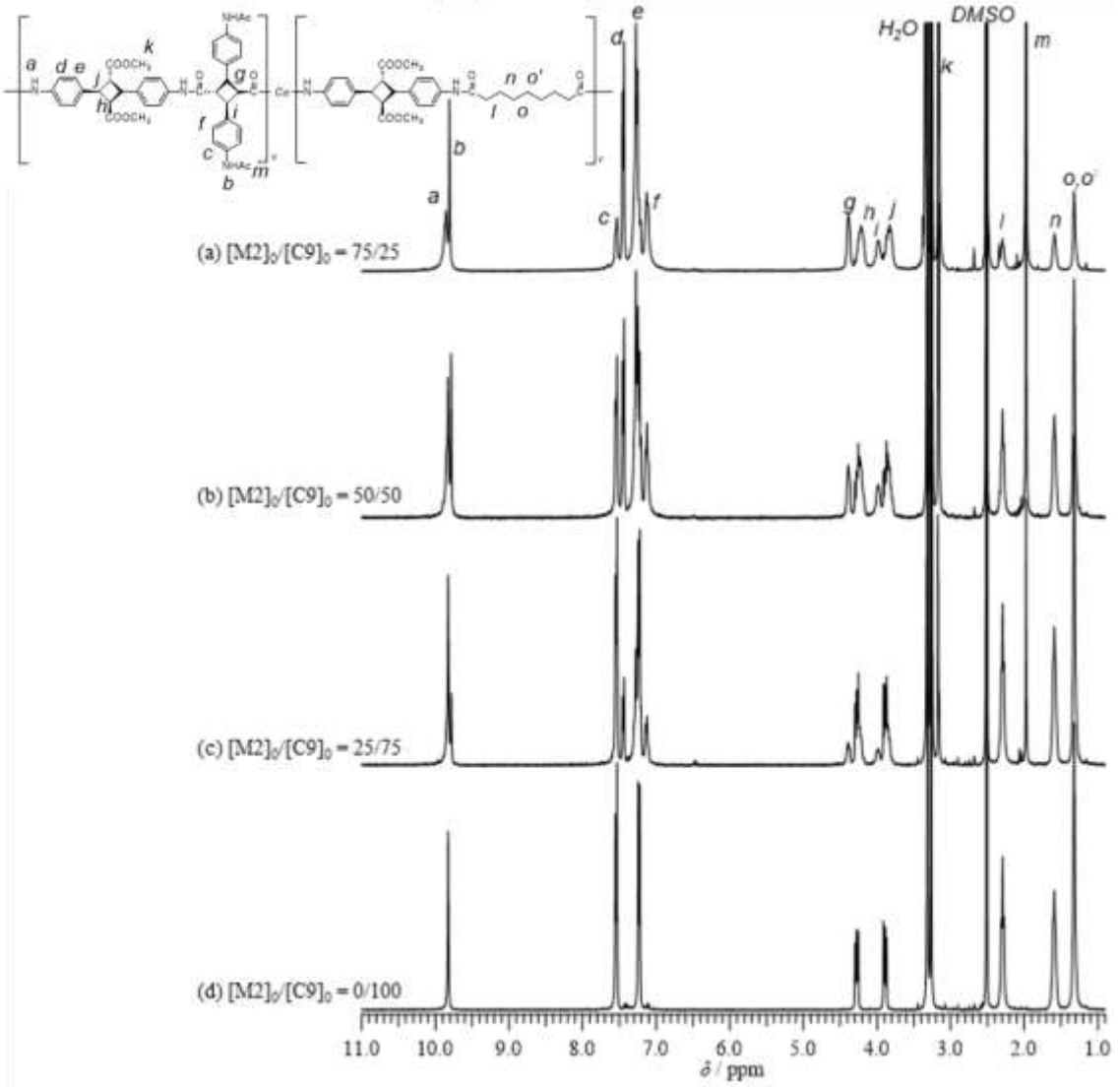

Figure 2-5. ^{1}H NMR spectra of PA-C9 with various monomer ratios $[M2]_0/[C9]_0$ (400MHz NMR; solvent, DMSO-d_6).

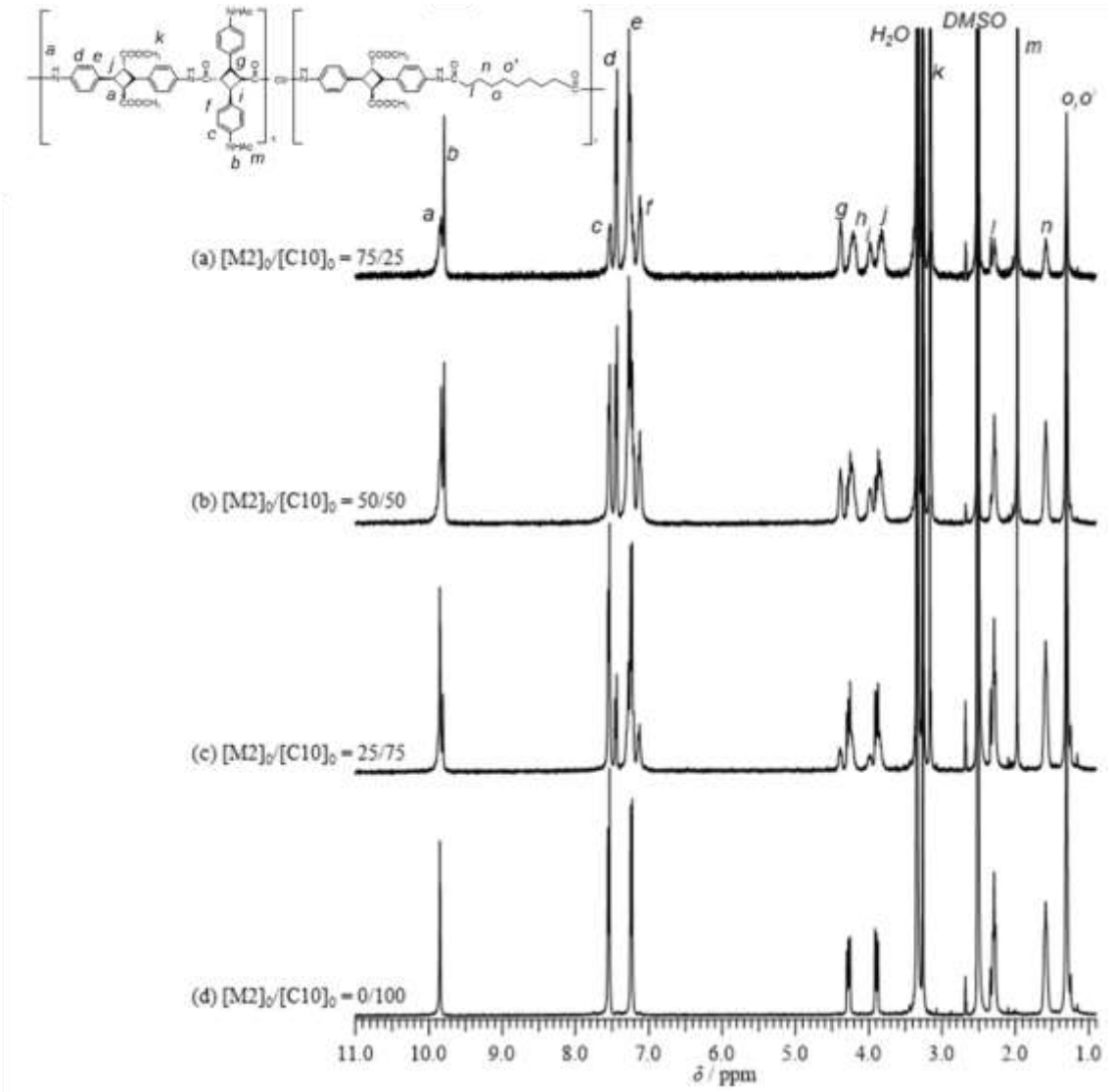

Figure 2-6. ^{1}H NMR spectra of PA-C10 with various monomer ratios $[M2]_0/[C10]_0$ (400MHz NMR; solvent, DMSO-d_6).

2.3.1 Properties of *co*-polyamides

To determine the solubility of the synthesized polyamides, small sample amounts (~5 mg) were added to test tubes with solvents (1.0 mL) such as methanol (CH_3OH),

tetrahydrofuran (THF), dimethyl sulfoxide (DMSO), *N*,*N*-dimethyl formamide (DMF), N-methyl-2-pyrrolidone (NMP), N,N-dimethyl acetamide (DMAc), trifluoroacetic acid (TFA), toluene, and chlorobenzene (C_6H_5Cl). The polyamides dissolved easily in DMSO, DMF, DMAc, and TFA, regardless of the aliphatic diacid composition (Table 2-1). DMF was used as the solvent for processing because it offered good solubility and safety.

Table 2-1. Solubility of PA-C6 with various monomer compositions at 20 °C[a]

$[M2]_0/[C6]_0$	CH_3OH	THF	DMSO	DMF	NMP	DMAc	TFA	Toluene	C_6H_5Cl
100/0 [b]	−	−	++	++	+	++	++	−	−
75/25	−	−	++	++	+	++	++	−	−
50/50	−	−	++	++	+	++	++	−	−
25/75	−	−	++	++	+	++	++	−	−
0/100	−	−	++	++	++	++	++	−	−

[a]Sample (PA-C6), 5 mg; solvent, 1.0 mL; solubility, ++ (immediately soluble), + (dissolved by ultrasonic agitation), − (insoluble). [b] Homo-polyamide (homo-PA) synthesized from M1 and M2.

The 5% (T_{d5}) and 10% (T_{d10}) degradation temperatures of the polyamides were approximately 345 and 360 °C, respectively. These values indicate that the aliphatic segment had negligible influence on T_{d5} and T_{d10}. However, the glass transition temperature (T_g) of polyamides was approximately 185 °C, which is lower than that of the homo-polyamide (270 °C). This indicates that the molecular flexibility of the polyamides was reinforced by the addition of the aliphatic segment. Furthermore, these T_g values are also higher than those of

common transparent plastics such as poly(lactic acid) (53–64 °C), poly(ethylene terephthalate) (69–115 °C), and polystyrene (100 °C). In addition, optical properties such as the yellow index and transparency at 400 and 450 nm were improved from the homo-polyamide by copolymerization with aliphatic diacids. The transparencies at 400 nm were shown approximately 80%, their values were almost the same at quartz glass (approximately 90%) or polystyrene (approximately 80%).[38] The properties of the synthesized polyamides are summarized in Table 2-2.

Table 2-2. Molecular weight, thermal properties, and optical properties of all the obtained *co*-polyamides and homo-biopolyamide[a]

Polymer	$[M2]_0/[Cn]_0$	$M_n \times 10^{5}$ [b]	$M_w \times 10^{5}$ [b]	PDI[b]	T_{d5}[c] (ºC)	T_{d10}[c] (ºC)	T_g[d] (ºC)	Yellow Index[e]	Transparency[e,f] (%) 400 nm	450 nm
homo-PA	100/0	1.7	5.8	3.2	351	368	270	10.6	67 (386 nm)	80
PA-C6	75/25	2.9	6.7	2.3	348	361	246	7.5	73 (396 nm)	84
	50/50	1.3	2.5	1.8	341	357	219	8.1	72 (374 nm)	83
	25/75	2.7	5.8	2.1	350	364	196	6.2	76 (373 nm)	86
	0/100	3.5	6.1	1.8	355	367	166	ND	ND	ND
PA-C7	75/25	3.1	7.7	2.4	353	366	245	10.0	69 (379 nm)	81
	50/50	3.4	7.7	2.3	352	365	220	5.5	78 (373 nm)	86
	25/75	3.9	10	2.6	353	365	191	4.8	81 (381 nm)	87
	0/100	ND	ND	ND	353	365	159	ND	ND	ND
PA-C8	75/25	2.5	5.1	2.0	334	347	244	8.9	69 (382 nm)	83
	50/50	2.8	5.6	2.0	340	353	220	8.6	70 (378 nm)	83
	25/75	2.5	4.9	2.0	337	350	191	9.6	66 (386 nm)	82
	0/100	ND	ND	ND	338	352	159	ND	ND	ND
PA-C9	75/25	2.6	6.5	2.4	338	353	245	6.4	77 (388 nm)	85
	50/50	2.4	4.7	2.0	337	352	214	5.3	80 (369 nm)	86
	25/75	1.8	3.4	1.9	341	354	176	6.1	79 (357 nm)	86
	0/100	1.6	2.9	1.8	337	351	137	ND	ND	ND
PA-C10	75/25	2.4	4.9	2.1	339	354	242	8.9	69 (403 nm)	83
	50/50	2.4	5.4	2.2	341	355	211	6.9	75 (372 nm)	85
	25/75	2.8	5.3	1.9	343	356	175	4.2	83 (358 nm)	87
	0/100	2.7	4.5	1.7	345	357	138	ND	ND	ND

[a]Polymerization conditions; $[M1]_0/([M2]_0+[Cn]_0)$, 100/100; solvent, NMP; temp., 80 °C; N_2 atmosphere. ND:Not detected. [b]Determined by gel permeation chromatography using 0.01 mol L^{-1} LiBr DMF solution, and polystyrene standards; flow rate, 1.0 mL min^{-1}. [c]Measured by TGA; heating rate, of 5 °C min^{-1}; N_2 atmosphere. [d]Measured by DSC; heating rate, of 10 °C min^{-1}; N_2 atmosphere. [e]Yellow Index and transparency at 400 nm and 450 nm were measured by spectrophotometry. [f]Cut off wavelength shown in second line of each.

Thus, it is evident that the addition of an aliphatic dicarboxylic acid as a comonomer to the bio-polyamide increased its amorphous region and improved its flexibility and transparency. The solubility tests revealed that DMF was a suitable solvent for the preparation of polyamide fibers. Thus, various polyamide fibers with monomer ratio of $[M2]_0/[Cn]_0$ 25/75 were obtained and their strength was measured by the tensile test (Table 2-3). The incorporation of aliphatic chains increased the elongation at break and reduced the Young's modulus. The maximum mechanical strength (σ_{MAX}) of the polyamides was 472 MPa on average and 534 MPa at maximum for PA-C7 $[M2]_0/[C7]_0$ of 75/25 (Figure 2-7A). To the best of my knowledge, this value of σ_{MAX} is the highest among all the amorphous and transparent organic materials.

Table 2-3. Mechanical properties of the obtained *co*-polyamides, homo-polyamide, and the representative fiber materials[a]

Material	$[M2]_0/[Cn]_0$	E (GPa)[b]	σ_{MAX} (MPa)[b]	ε (%)[b]	U_d[c] (MJ m^{-3})[b]
homo-PA	100/0	9.7 ± 1.0	321 ± 27	32 ± 3	66 ± 7
PA-C6	75/25	8.4 ± 1.3	322 ± 23	56 ± 1	104 ± 10
	50/50	10.2 ± 1.5	344 ± 67	46 ± 8	105 ± 14
	25/75	6.4 ± 0.9	333 ± 32	95 ± 6	133 ± 17
PA-C7	75/25	9.3 ± 0.9	472 ± 46	61 ± 2	155 ± 15
	50/50	7.7 ± 2.4	289 ± 35	88 ± 4	131 ± 12
	25/75	5.8 ± 0.6	322 ± 15	117 ± 9	218 ± 18
PA-C8	75/25	9.4 ± 1.3	388 ± 11	60 ± 3	141 ± 14
	50/50	6.9 ± 1.3	321 ± 18	87 ± 6	155 ± 5
	25/75	7.1 ± 1.6	354 ± 69	118 ± 7	231 ± 58
PA-C9	75/25	9.2 ± 1.1	418 ± 45	59 ± 5	140 ± 16
	50/50	7.9 ± 0.7	352 ± 36	75 ± 14	152 ± 28
	25/75	4.4 ± 0.6	244 ± 26	134 ± 9	190 ± 28
PA-C10	75/25	8.6 ± 0.9	366 ± 37	60 ± 2	149 ± 15
	50/50	5.4 ± 0.3	255 ± 43	95 ± 3	132 ± 28
	25/75	4.4 ± 0.5	267 ± 57	137 ± 15	170 ± 28
High tensile strength steel		200	1500	0.8	6
Kevlar[a]		130	3600	2.7	50
Silicon rubber		0.001	50	850	100
Spider silk[c]		8.8	878	20.0	107
(*Nephila clavate*)		(13.8)	(1215)	(17.2)	(111)

[a]All materials were measured as fibers; monomer ratio of *co*-polyamides, $[M1]_0/([M2]_0+[Cn]_0)$, 100/100; (homo-polyamide, $[M1]_0/[M2]_0$ = 100/100/0). [b]Mechanical properties, E, σ, ε, and U_d were measured by tensile tests at 0.50 mm min^{-1} of tension rate. [c]Average value of the spider silk and the value in parentheses are *Nephila clavate.*

Additionally, PA-C7 showed a high toughness of 155 MJ m^{-3} on average (184 MJ m−3 at maximum) compared to representative fiber materials shown in the lower part of Table 2-3, such as high-tensile strength steel, Kevlar, silicon rubber, and spider silk (average value and silk of Nephila clavata, a spider commonly found in Japan). Further increase in the content of aliphatic chains $[M2]_0/[Cn]_0$ to 25/75 increased the toughness remarkably (Figure 2-7 B). In particular, the PA with $[M2]_0/[C8]_0$ composition of 25/75 had the maximum toughness of 231 MJ m^{-3}, which is much higher than that of spider silk as well as synthetic fibers. It showed a toughness of 340 MJ m^{-3} at maximum, which is comparable to that of Darwin's bark spider silk.

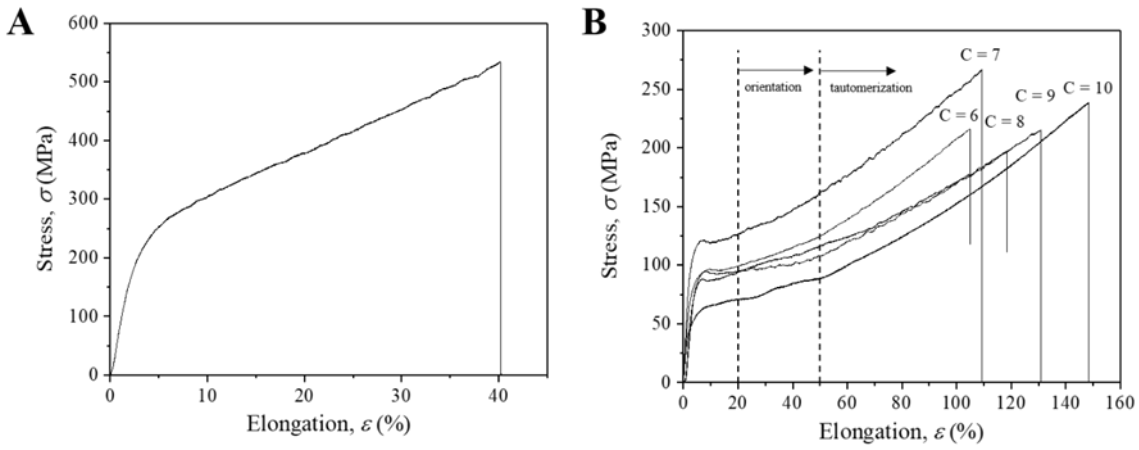

Figure 2-7. (A) Stress–strain curve of PA-C7 with $[M2]_0/[C7]_0$ monomer ratio of 75/25. (B) Stress–strain curves of polyamides with $[M2]_0/[Cn]_0$ monomer ratio of 25/75.

2.3.2 Structural Analysis of *co*-polyamide fibers

To clarify the mechanism of superhigh toughness and strength, *in situ* measurements were carried out using the PA-C10 specimen, which showed the highest elongation of all the prepared polyamides.

In situ XRD measurements were carried out to check the orientation and crystallization of polyamides using wide-angle XRD (2D-WAXD) images (Figure 2-8A). As a result of orientation analyses (Figure 2-8B), the orientation degree increased with increasing elongation from 20% to 60% and then remained constant at ~0.4–0.5. No crystalline diffractions appeared in the 2D-WAXD image due to elongation. Further, from the differential scanning calorimeter (DSC) measurement it was found that the peaks corresponding to the melting point was not observed in any of the polyamides; therefore, the polyamides can be considered as amorphous.

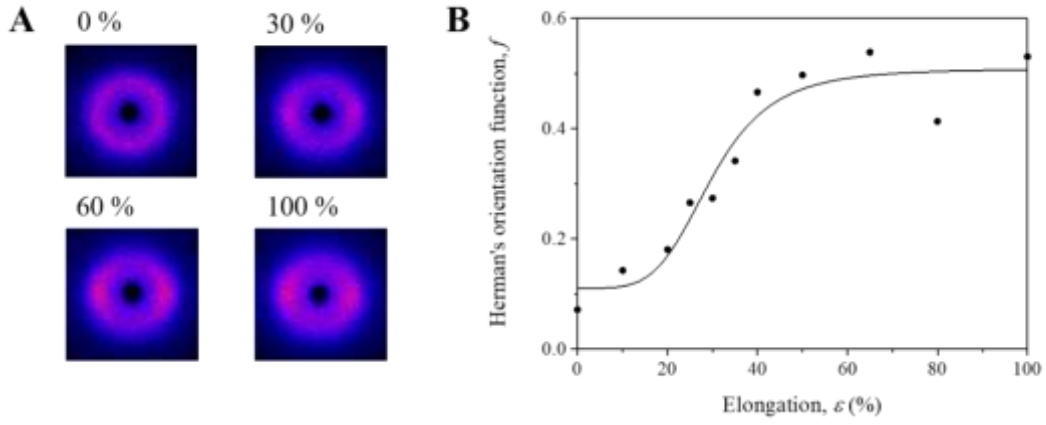

Figure 2-8. (A) 2D-WAXD images of PA-C10 ($[M2]_0/[C7]_0$, 25/75) at several elongations. (B)

Orientation behavior through the tensile test calculated using Eq. 2. Exposure time,180 s (+ 300 s from 40 % elongation); elongation range, 0 % ~ 100 %.

Additional *in situ* measurements using FT-IR were performed for functional group analysis under elongation (Figure 2-9A). As a result of differential IR analyses (Figure 2-9B), it was found that two new peaks corresponding to C=C double bond and C=N imine bond were observed at ~1690 cm^{-1}, respectively, in the IR spectrum of 65% elongated PA-C10 $[M2]_0/[C10]_0$ of 25/75. From these observations, it was assumed that tautomerization occurs where the C=C of cyclobutadiene and C=N of the amide linkage is formed (Figure 2-9C). In particular, protons of cyclobutane can be transferred to the neighboring ester in the diamine moiety and to the neighboring amide in the diacid, which converts cyclobutane to cyclobutadiene. Such tautomerization can occur under ambient conditions, but the cyclobutane structure is more stable. On the other hand, when strong tension is applied to the polyamide chains, the planar structure is stabilized to enhance the tautomerization to cyclobutadiene, which has a higher modulus than cyclobutane.

The *co*-polyamides were easily stretched by applying an external force along its direction without major stress concentration because the aliphatic moiety of polyamides was mainly oriented along the force direction (Figure 2-9C, 1st stage). After the aliphatic moiety

was sufficiently extended, the orientation function was saturated at approximately 50 % elongation, which resulted in stress concentration throughout the structure. The tautomerization process hardened the stressed zone to induce snap-buckling at a molecular level of higher than 50 % elongation. The present series of polyamides showed remarkable elongation despite the aromatic/alicyclic rigid main-chains, like a molecular spring. The enhancement of the mechanical strength throughout the tensile test could be explained by orientation and tautomerization-induced hardening (Figure 2-9C, 2nd stage). As a consequence, polyamides with a higher ratio of aliphatic dicarboxylic acids maintained their mechanical strength with increasing elongation, resulting in exceptional toughness as fiber materials.

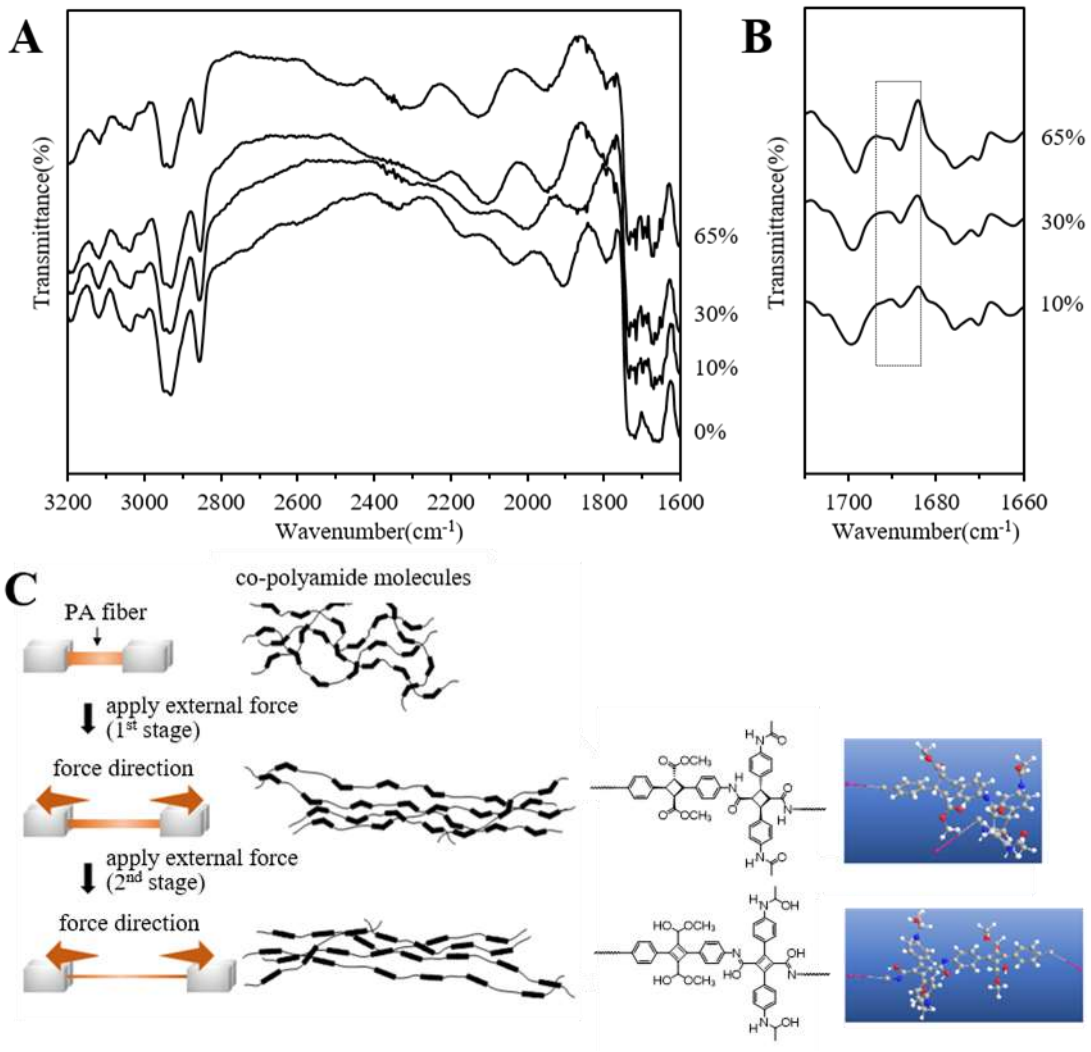

Figure 2-9. (A) FT-IR spectra of PA-C10 at different elongation. (B) Differential FT-IR spectra of PA-C10 at 10%, 30%, and 65%. Elongation cumulative number, 8 times; wavenumber range, 700 cm^{-1} ~ 4000 cm^{-1}; elongation range, 0 % ~ 65 %. (C)Schematic illustration of tautomerization of polyamide fiber while applying external force. At the 1st stage (approximately 50 % elongation), aliphatic main chain was oriented along the direction of applied force, while cyclobutane retained its twisted shape. At the 2nd stage (higher than 50 % elongation), tautomerization of main chain cyclobutane was enhanced with increase in force

to form a planar main chain including cyclobutadiene and imine bond.

2.3.3 Self-standing nanomembranes

Polyamide nano coatings, PA-C8, were obtained by spin- coating on a glass substrate using a DMF solution. As shown in Figure 2-10A, the nanocoat exhibited few rings with interference colors, implying that the coating thickness is at sub-micrometer scale. The nanomembranes were successfully peeled away from the glass substrate without breaking from the coat periphery by a paper-supported double-sided tape owing to their high toughness (Figure 2-10B). Consequently, a nanomembrane with a thickness of ~200 nm was formed, which displayed interference colors (Figure 2-10C). The nanomembranes were self-standing, although they were thinner than expected, as shown in Figure 2-10D. In addition, the refractive indices, n, ranged from 1.64 to 1.87 depending on the light wavelength (Abbe's number v_d = 43), and were much higher than that of the glass plate under visible light (n = 1.55–1.62) (Figure 2-11). These results suggest that the polyamide membranes should be supertough enough to use as self-standing nanomaterials for flexible and/or miniaturized devices.

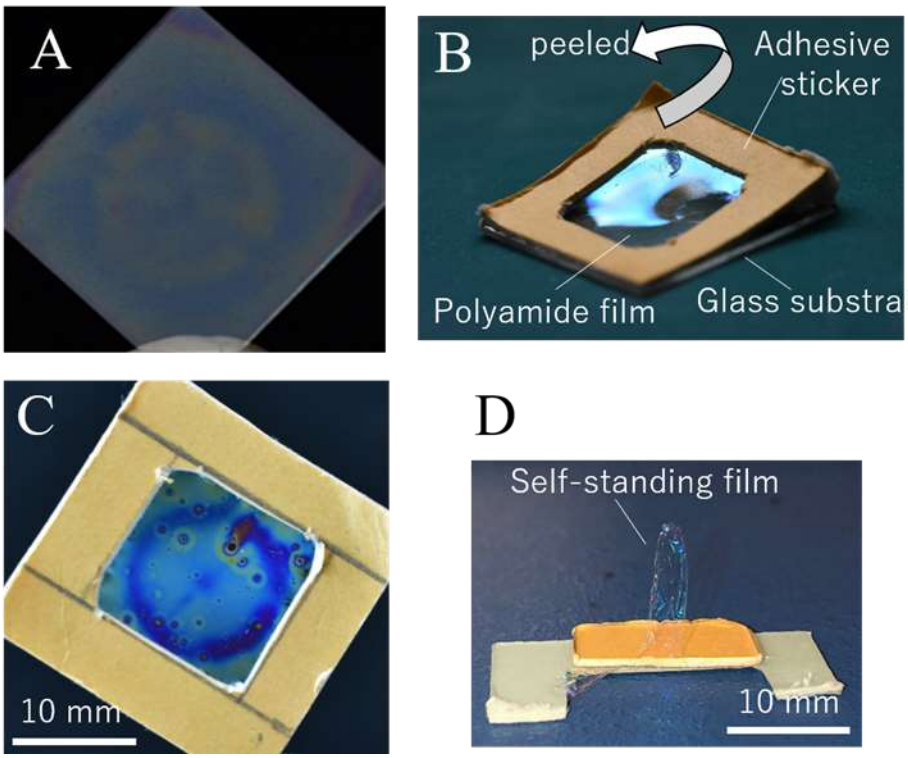

Figure 2-10. Pictures of the PA-C8 ([M2]$_0$/[C8]$_0$, 25/75) nanomembrane. (A) Spin-cast membrane on a glass plate. (B) Nanomembrane peeling out of glass plate. (C) After peeling. (D) Self-standing nanomembrane.

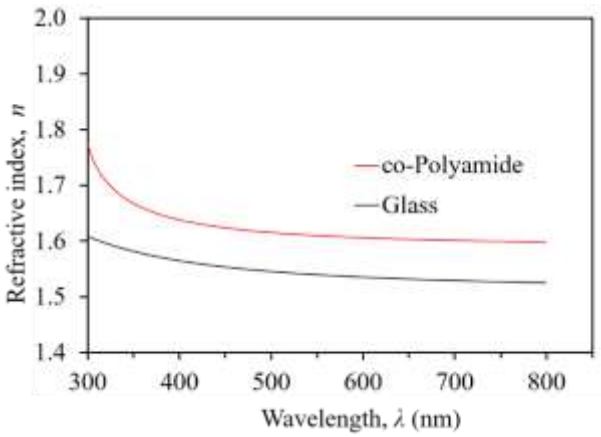

Figure 2-11. Refractive index curves of the PA-C8 nanomembrane ([M2]$_0$/[C8]$_0$, 25/75) and

glass plate for comparison.

2.4 Conclusion

Self-standing membrane even with a nanoscale thickness were developed by spin-cast of polyamides with ultra-high mechanical strength and toughness. The polyamides were designed by the polycondensation of diamine and diacid derivatives of *α*-truxillic acid, which is a photodimer of bio-based 4ACA, in the presence of aliphatic dicarboxylic acids as comonomers. In the presence of 25 mol% of pimelic acid, the synthesized polyamides possessed a mechanical strength of 470 MPa, which is the highest value reported to date for an amorphous organic material. In addition, another polyamide synthesized in the presence of 75 mol% of suberic acid was found to be super-tough with a mechanical strength of 230 MJ m^{-3}, which exceeds that of conventional fiber materials, including almost all spider webs. These exceptional mechanical properties were attributed to the orientation and tautomerization, and the conversion of non-planar cyclobutane to planar and rigid cyclobutadiene, which was stabilized under strong tension, as confirmed by *in situ* FT-IR measurements. This conversion can induce snap-buckling like a molecular spring and enhance mechanical strength and toughness, which were higher in the synthesized polyamides as compared to those of spider silk. The nanomembrane was spin-cast to self-stand after peeling away from the glass plate. The present results suggest that the

nanomembrane can be innovative to open a new field of thin flexible materials for electronic displays, organic memory, and other devices, and to contribute to miniaturized machines such as mini-robots working *in vivo*.

REFERENCES

1. Makabe, H.; Banba, T.; Hirano, T., A Novel Positive Working Photosensitive Polymer For Semiconductor Surface Coating. *Journal of Photopolymer Science and Technology* **1997,** *10* (2), 307-311.

2. Turchanin, A.; Gölzhäuser, A., Carbon Nanomembranes. *Advanced Materials* **2016,** *28* (29), 6075-6103.

3. Rogers, J. A.; Lagally, M. G.; Nuzzo, R. G., Synthesis, assembly and applications of semiconductor nanomembranes. *Nature* **2011,** *477* (7362), 45-53.

4. Watanabe, H.; Muto, E.; Ohzono, T.; Nakao, A.; Kunitake, T., Giant nanomembrane of covalently-hybridized epoxy resin and silica. *Journal of Materials Chemistry* **2009,** *19* (16), 2425-2431.

5. Okamura, Y.; Kabata, K.; Kinoshita, M.; Saitoh, D.; Takeoka, S., Free-Standing Biodegradable Poly(lactic acid) Nanosheet for Sealing Operations in Surgery. *Advanced Materials* **2009,** *21* (43), 4388-4392.

6. Fujino, K.; Kinoshita, M.; Saitoh, A.; Yano, H.; Nishikawa, K.; Fujie, T.; Iwaya, K.;

Kakihara, M.; Takeoka, S.; Saitoh, D.; Tanaka, Y., Novel technique of overlaying a poly-l-lactic acid nanosheet for adhesion prophylaxis and fixation of intraperitoneal onlay polypropylene mesh in a rabbit model. *Surgical Endoscopy* **2011,** *25* (10), 3428.

7. Miyazaki, H.; Kinoshita, M.; Saito, A.; Fujie, T.; Kabata, K.; Hara, E.; Ono, S.; Takeoka, S.; Saitoh, D., An ultrathin poly(L-lactic acid) nanosheet as a burn wound dressing for protection against bacterial infection. *Wound Repair Regen* **2012,** *20* (4), 573-9.

8. Pensabene, V.; Taccola, S.; Ricotti, L.; Ciofani, G.; Menciassi, A.; Perut, F.; Salerno, M.; Dario, P.; Baldini, N., Flexible polymeric ultrathin film for mesenchymal stem cell differentiation. *Acta Biomaterialia* **2011,** *7* (7), 2883-2891.

9. Meyerbröker, N.; Zharnikov, M., Ultraflexible, Freestanding Nanomembranes Based on Poly(ethylene glycol). *Advanced Materials* **2014,** *26* (20), 3328-3332.

10. Fujie, T.; Desii, A.; Ventrelli, L. Mazzolai, B.; Mattoli, V., Inkjet printing of protein microarrays on freestanding polymeric nanofilms for spatio-selective cell culture environment. *Biomedical Microdevices* **2012,** *14* (6), 1069-1076.

11. Zhang, H.; Takeoka, S., Morphological Evolution within Spin-Cast Ultrathin Polymer Blend Films Clarified by a Freestanding Method. *Macromolecules* **2012,** *45* (10), 4315-4321.

12. Hasegawa, H.; Ohta, T.; Ito, K.; Yokoyama, H., Stress-strain measurement of ultra-thin polystyrene films: Film thickness and molecular weight dependence of crazing stress.

Polymer **2017,** *123*, 179-183.

13. Roberts, M. M.; Klein, L. J.; Savage, D. E.; Slinker, K. A.; Friesen, M.; Celler, G.; Eriksson, M. A.; Lagally, M. G., Elastically relaxed free-standing strained-silicon nanomembranes. *Nature Materials* **2006,** *5* (5), 388-393.

14. Pérez-Madrigal, M. M.; Armelin, E.; Puiggalí, J.; Alemán, C., Insulating and semiconducting polymeric free-standing nanomembranes with biomedical applications. *Journal of Materials Chemistry B* **2015,** *3* (29), 5904-5932.

15. Puiggalí-Jou, A.; Molina, B. G.; Lopes-Rodrigues, M.; Michaux, C.; Perpète, E. A.; Zanuy, D.; Alemán, C., Self-standing, conducting and capacitive biomimetic hybrid nanomembranes for selective molecular ion separation. *Physical Chemistry Chemical Physics* **2021,** *23* (30), 16157-16164.

16. Bower, G. M.; Frost, L. W., Aromatic polyimides. *Journal of Polymer Science Part A: General Papers* **1963,** *1* (10), 3135-3150.

17. Sezer Hicyilmaz, A.; Celik Bedeloglu, A., Applications of polyimide coatings: a review. *SN Applied Sciences* **2021,** *3* (3), 363.

18. García, J. M.; García, F. C.; Serna, F.; de la Peña, J. L., High-performance aromatic polyamides. *Progress in Polymer Science* **2010,** *35* (5), 623-686.

19. Reglero Ruiz, J. A.; Trigo-López, M.; García, F. C.; García, J. M., Functional

Aromatic Polyamides. *Polymers* **2017,** *9* (9), 414.

20. Dwivedi, S.; Nag, A.; Sakamoto, S.; Funahashi, Y.; Harimoto, T.; Takada, K.; Kaneko, T., High-temperature resistant water-soluble polymers derived from exotic amino acids. *RSC Advances* **2020,** *10* (62), 38069-38074.

21. Kato, S.; Amat Yusof, F. A.; Harimoto, T.; Takada, K.; Kaneko, T.; Kawai, M.; Mitsumata, T., Electric Volume Resistivity for Biopolyimide Using 4,4'-Diamino-alpha-truxillic acid and 1,2,3,4-Cyclobutanetetracarboxylic dianhydride. *Polymers (Basel)* **2019,** *11* (10).

22. Takada, K.; Karikome, S.; Dwivedi, S.; Kaneko, T., Fully Bio-based Aromatic Polyimide Using 4-Aminocinnamic Acid and Mellophanic Dianhydride as Bio-derived Monomers. *ECS Transactions* **2018,** *88* (1), 99-105.

23. Dwivedi, S.; Kaneko, T., Robustification of ITO nanolayer by surface-functionalization of transparent biopolyimide substrates. *Journal of Applied Polymer Science* **2018,** *135* (40).

24. Shin, H.; Wang, S.; Tateyama, S.; Kaneko, D.; Kaneko, T., Preparation of a Ductile Biopolyimide Film by Copolymerization. *Industrial & Engineering Chemistry Research* **2016,** *55* (32), 8761-8766.

25. Huang, T. T.; Tsai, C. L.; Tateyama, S.; Kaneko, T.; Liou, G. S., Highly transparent and flexible bio-based polyimide/TiO_2 and ZrO_2 hybrid films with tunable refractive index,

Abbe number, and memory properties. *Nanoscale* **2016,** *8* (25), 12793-802.

26. Suvannasara, P.; Tateyama, S.; Miyasato, A.; Matsumura, K.; Shimoda, T.; Ito, T.; Yamagata, Y.; Fujita, T.; Takaya, N.; Kaneko, T., Biobased Polyimides from 4-Aminocinnamic Acid Photodimer. *Macromolecules* **2014,** *47* (5), 1586-1593.

27. Phanthuwongpakdee, J.; Babel, S.; Dwivedi, S.; Takada, K.; Hirayama, T.; Kaneko, T., Anion-Scavenging Biopolyamides from Quaternized 4-Aminocinnamic Acid Photodimers. *ACS Sustainable Chemistry & Engineering* **2020,** *8* (9), 3786-3795.

28. Takada, K.; Mae, Y.; Kaneko, T., Fluorinated and Bio-Based Polyamides with High Transparencies and Low Yellowness Index. *Polymers (Basel)* **2018,** *10* (12).

29. Tateyama, S.; Masuo, S.; Suvannasara, P.; Oka, Y.; Miyazato, A.; Yasaki, K.; Teerawatananond, T.; Muangsin, N.; Zhou, S.; Kawasaki, Y.; Zhu, L. Zhou, Z.; Takaya, N.; Kaneko, T., Ultrastrong, Transparent Polytruxillamides Derived from Microbial Photodimers. *Macromolecules* **2016,** *49* (9), 3336-3342.

30. Froidevaux, V.; Negrell, C.; Caillol, S.; Pascault, J. P.; Boutevin, B., Biobased Amines: From Synthesis to Polymers; Present and Future. *Chem Rev* **2016,** *116* (22), 14181-14224.

31. Isikgor, F. H.; Becer, C. R., Lignocellulosic biomass: a sustainable platform for the production of bio-based chemicals and polymers. *Polymer Chemistry* **2015,** *6* (25), 4497-

4559.

32. Beach, E. S.; Cui, Z.; Anastas, P. T., Green Chemistry: A design framework for sustainability. *Energy & Environmental Science* **2009,** *2* (10).

33. Miller, S. A., Sustainable Polymers: Opportunities for the Next Decade. *ACS Macro Letters* **2013,** *2* (6), 550-554.

34. Torres, N.; Robin, J. J.; Boutevin, B., Study of thermal and mechanical properties of virgin and recycled poly(ethylene terephthalate) before and after injection molding. *European Polymer Journal* **2000,** *36* (10), 2075-2080.

35. Ali, U.; Karim, K. J. B. A.; Buang, N. A., A Review of the Properties and Applications of Poly (Methyl Methacrylate) (PMMA). *Polymer Reviews* **2015,** *55* (4), 678-705.

36. Bagotia, N.; Choudhary, V.; Sharma, D. K., A review on the mechanical, electrical and EMI shielding properties of carbon nanotubes and graphene reinforced polycarbonate nanocomposites. *Polymers for Advanced Technologies* **2018,** *29*, 1547-1567.

37. Saxon, D. J.; Luke, A. M.; Sajjad, H.; Tolman, W. B.; Reineke, T. M., Next-generation polymers: Isosorbide as a renewable alternative. *Progress in Polymer Science* **2020,** *101*, 101196.

38. Nunes, P. S.; Ohlsson, P. D.; Ordeig, O.; Kutter, J. P., Cyclic olefin polymers: emerging materials for lab-on-a-chip applications. *Microfluidics and Nanofluidics* **2010,** *9* (2),

145-161.

39. Kwon, G.; Lee, K. Kim, D.; Jeon, Y.; Kim, U.-J.; You, J., Cellulose nanocrystal-coated TEMPO-oxidized cellulose nanofiber films for high performance all-cellulose nanocomposites. *Journal of Hazardous Materials* **2020,** *398*, 123100.

40. Agnarsson, I.; Kuntner, M.; Blackledge, T. A., Bioprospecting Finds the Toughest Biological Material: Extraordinary Silk from a Giant Riverine Orb Spider. *PLOS ONE* **2010,** *5* (9), e11234.

41. Gosline, J. M.; Guerette, P. A.; Ortlepp, C. S.; Savage, K. N., The mechanical design of spider silks: from fibroin sequence to mechanical function. *Journal of Experimental Biology* **1999,** *202* (23), 3295-3303.

42. Swanson, B. O.; Blackledge, T. A.; Beltrán, J.; Hayashi, C. Y., Variation in the material properties of spider dragline silk across species. *Applied Physics A* **2006,** *82* (2), 213-218.

43 [a] R. H. Somani, L Yang, B. S. Hsiao, T. Sun, N. V. Pogodina and A. Lustiger, Shear-Induced Molecular Orientation and Crystallization in Isotactic Polypropylene: Effects of the Deformation Rate and Strain. *Macromolecules* 2005, **38**, 1244-1255. [b] E. Loizou, L. Porcar, P. Schexnailder, G. Schmidt and P. Butler, *Macromolecules* 2010, **43**, 1041-1049.

Chapter 3. Water-solubilization/ Insolubilization of polyamide

3.1 Introduction and research background

Polyamides, well known as engineering plastics, are widely used automotive parts, fibers or electronic com components use of its toughness or thermal resistance. But on the other hand, most polyamides have low processability because of their high toughness and high molding temperature.[1-4] Especially, Kevlar the aromatic polyamide extremely difficult to process so its processing is realized by using concentrated sulfuric acid.[5,6] Kaneko laboratory have previously reported 4-amino cinnamic acid-based aromatic polyimides. [7-11]The polyamides have shown solubility to only high-boiling solvents such as *N*-methyl-2-pyroridone, *N*,*N*-dimethylacetamide, *N*,*N*-dimethylformamide, dimethyl sulfoxide and concentrated sulfuric acid.[11]

One of method of improving processability without degrading heat resistance is to control the solubility. Water has lower boiling point than sulfuric acid or high-boiling solvents such as dimethyl sulfoxide. Furthermore, water is attracting attention as environment-friendly solvent for painting and coating.[12-14]

On the other hand, Cellulose Nano Fibers (CNF) have also received attention as environment-friendly material. CNF is a biomass material produced from plants, and has been actively studied because of characteristic properties such as high strength or high transparency etc.[15-18] CNF is considered that is compatible with hydrophilic materials

because it has widely appeared on the market as water dispersion liquid.

In this chapter, I focused on Water-solubilization and Insolubilization of 4-amino cinnamic acid-based polyamide using various metal ions. In addition, transparent composite films water-soluble polyamide and CNF.

3.2 Experimental

3.2.1Materials

Dimethyl sulfoxide, sodium hydride potassium hydroxide, magnesium chloride hexahydrate and calcium chloride dehydrate were purchased from Kanto Chemical Co., Inc. Ethanol was purchased Japan alcohol trading company Ltd. Cesium hydroxide mono hydrate was purchased Alfa Aesar. Strontium chloride hexahydrate and barium chloride dehydrate were purchased from FUJIFILM Wako Pure Chemical Corporation.

1.2% CNF aqueous dispersion was used as received from Oji Holding Co.

3.2.2 Syntheses of water-soluble polyamides

Bio-based *co*-polyamides were synthesized from 4-aminocinnamic acid-dimers, dimethyl 4,4'-diamino-*α*-truxillic acid and 4,4'-diacetoamide-*α*-truxillic acid, and suberic acid according to the previous literature.[11] Water-solubilization of *co*-polyamides were carried out by hydrolysis the methyl ester in the side chain of polyamide (Scheme 2-1). Synthetic procedure of K-type polyamide was follows. *Co*-polyamide (200 mg) was dissolved in

dimethyl sulfoxide (2 mL). After dissolved, 3 mol L^{-1} KOH aqueous solution (120 μL) was dripped to the solution and stirred for 12 hours at 20°C. After the reactions, reaction mixture was reprecipitated to large amount of ethanol (100 mL), after dry under vacuum at 150 °C to obtain the objective water-soluble *co*-polyamide. For preparation of *co*-polyamide films were carried out by solution casting method. A *co*-polyamide (100 mg) was dissolved to distilled water (3 mL) and cast to petri dish. Water was dried by standing for 2 days at 20°C, and the transparency film was obtained as COOK-type polyamide (WSPA-K) (Yield, 88.5 mg, 88.5%). As the water-soluble polyamides of other cation side chain, NaOH and CsOH were used instead of KOH by the same method as described above, and COO-Na type and COOCs-type polyamides (WSPA-Na and WSPA-Cs) were obtained in quantitative yields.

3.2.3 Insolubilization of polyamides

Water-soluble *co*-polyamides were insolubilized by the following method. WSPA-K was cut into square as 40 × 40 mm and immersed into 1.0 mol L^{-1} of aqueous solution of alkaline earth metal chloride, such as $MgCl_2$, $CaCl_2$, $SrCl_2$ or $BaCl_2$ as divalent cation. After immersed for 30 minutes, the film was washed by distilled water and dried at room temperature to give a cross-linked polyamides as ISPA-Mg ($MgCl_2$), ISPA-Ca ($CaCl_2$,), ISPA-Sr ($SrCl_2$) and ISPA-Ba ($BaCl_2$).

Scheme 3-1. Water solubilization of 4-aminocinnamic acid-based *co*-polyamide.

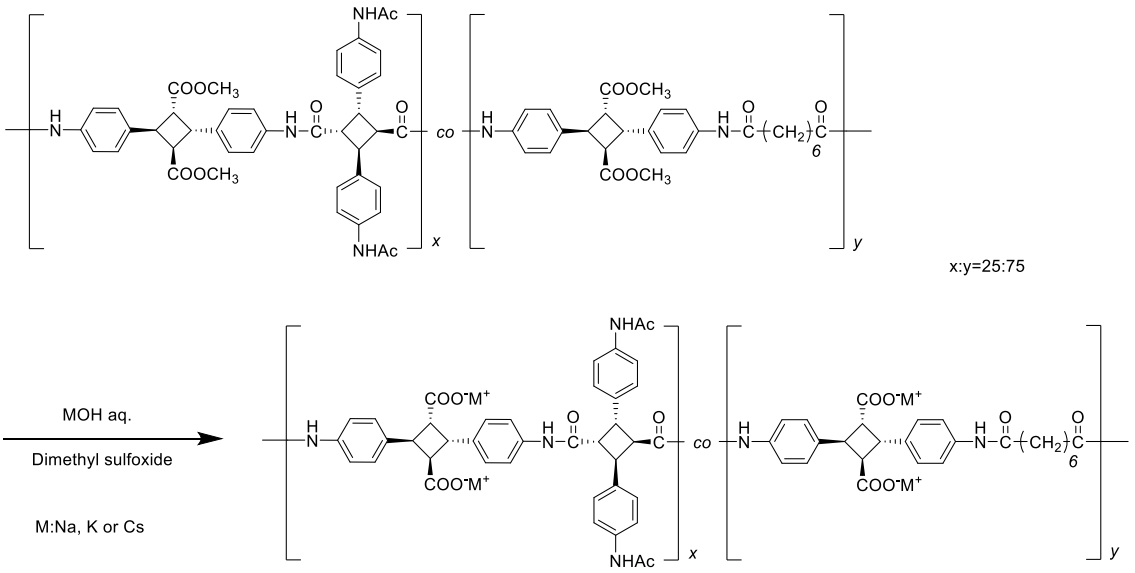

3.2.4 Preparation of composite films

CNF/WSPA composite films were prepared by the following method. Incidentally, WSPA-K was used for composites because its mechanical properties were highest.

Preparation procedures was follows. WSPA-K fibril was added to CNF aqueous dispersion and stirred until WSPA were dissolved to reach the ratio of CNF 0.5,1,5, 10, 20, 50 or 70 wt% in the dry state. After got viscus liquid, water added and more stirred to decrease viscosity. The liquid cast to glass petri dish and dried by standing for 2 days at 20°C.

3.2.5 Characterization

Nuclear magnetic resonance (NMR) spectra (^{1}H at 400 MHz) were obtained by an AVANCE III HD NMR spectrometer 400 MHz (BRUKER) using D_2O as a solvent. Thermal gravimetrical analysis (TGA) was carried out by STA 7200 (HITACHI) under nitrogen flow

(flow rate, 200mL min^{-1}) from 25 °C to 800 °C at heating rate of 5 °C min^{-1}. Differential scanning calorimeter (DSC) was performed by SEIKO X-DSC7000T to measured glass transition temperature (T_g) which were measured from 25 °C to a predetermined temperature that 5 °C lower than 1% degradation temperature (T_{d1}) at a heating rate of 10 °C min^{-1} (hold 5 min the predetermined temperature) with 5 mg sample. Mechanical properties of polymers were measured by using a tensile testing machine (Series 3360 Load Frame, Instron) with 0.50 mm min^{-1} as tension rate. Ultraviolet-Visible Absorption Spectroscopy (UV-Vis) was performed by V-670 (JASCO) in 250 nm to 800 nm as measured range. Fourier transform infrared spectroscopy (FT-IR) measurement was carried out using Spectrum 100 and Spectrum Spotlight 200 (Perkin Elmer) by Attenuated Total Reflection method. The obtained samples were observed by polarization microscope (POM) and Transmission Electron Microscope (TEM) H-7650 (HITACHI).

3.3 Results and discussion

To determine the solubility of WSPAs, small amounts were added to test tubes with solvents (1.0 mL) such as water, methanol, ethanol, hexane, tetrahydrofuran, *N*-methyl-2-pyroridone, *N*,*N*-dimethylacetamide (DMAc), *N*,*N*-dimethylformamide (DMF), dimethyl sulfoxide (DMSO) and concentrated sulfuric acid. The previously reported 4ACA-based polyamides were soluble in DMF, DMSO, DMAc, and NMP and showed no solubility in water.

However, by substituting side chains of bio-based polyamides with various alkali metal cation, this solubility was lost and instead exhibited solubility in water and methanol (Table 3-1).

Under similar conditions, lithium hydroxide was used as a catalyst, but the reaction did not proceed satisfactorily by the way. This is considered to be because lithium hydroxide is a relatively weak alkali.

Table 3-1. Solubility of polyamide alkali metal salts.[a]

Type	Water	MeOH	EtOH	Hexane	THF	NMP	DMAc	DMF	DMSO	conc H_2SO_4
Me	-	-	-	-	-	+	+	+	+	+
Na	+	+	-	-	-	-	-	-	-	+
K	+	+	-	-	-	-	-	-	-	+
Cs	+	+	-	-	-	-	-	-	-	+

[a]Sample, 5 mg; solvent, 1.0 mL; solubility, + (soluble), − (insoluble).

^{1}H NMR spectra of WSPAs were shown in figure 3-1. Structure and were confirmed by these spectra. The FT-IR spectra were shown in Figure 3-2. The spectrum of *co*-PA showed a peak assigned to the methyl ester group, 1750 cm^{-1} (C=O stretching). On the other hand, the peak was not determined in the spectra of WSPAs, indicated that saponification of methyl ester of side chain proceeded in any case. Incidentally, the peaks at 1650 cm^{-1} of amide were shown in any spectra.

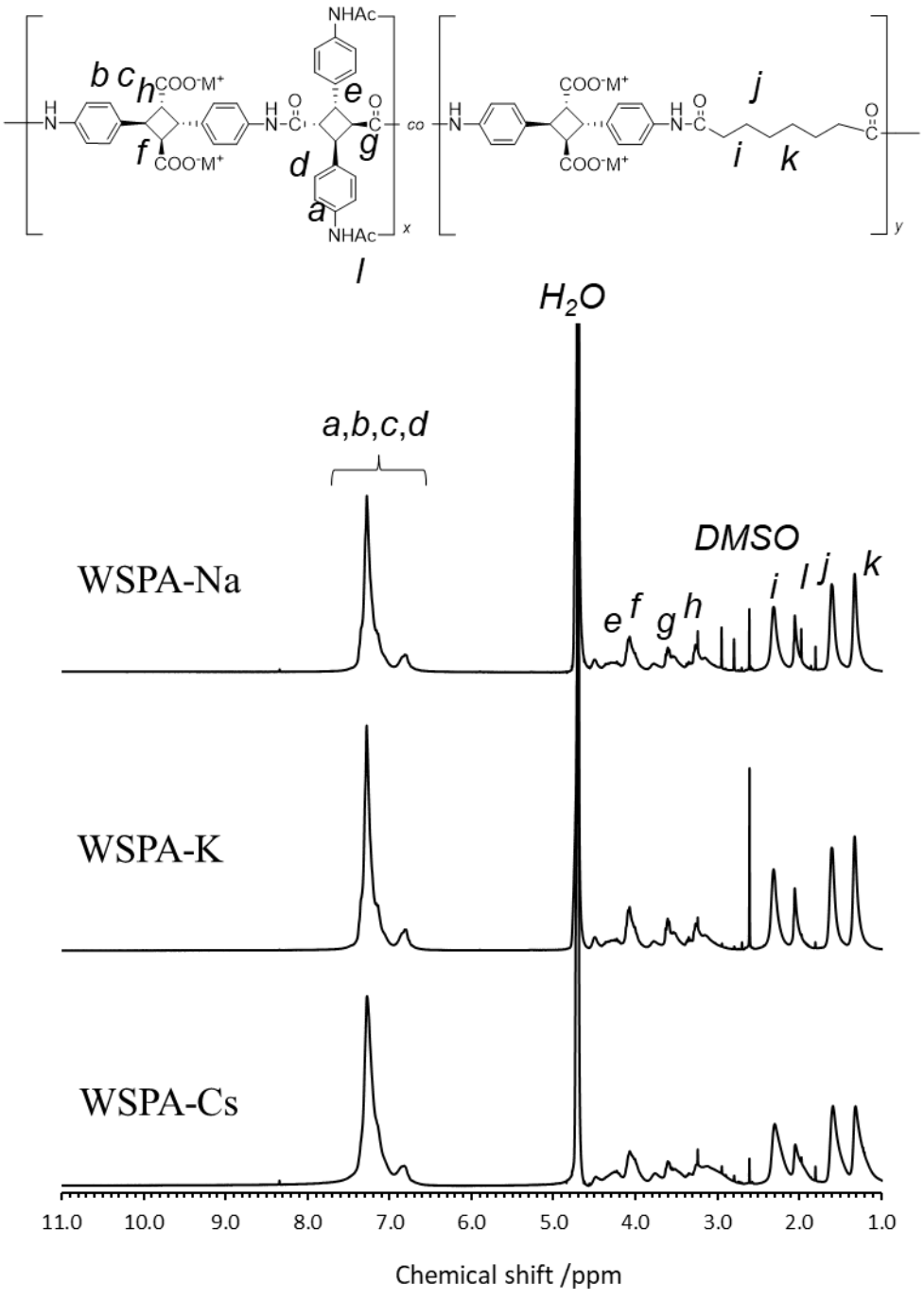

Figure 3-1. ^{1}H NMR spectra of WSPAs (400MHz NMR; solvent, D_2O).

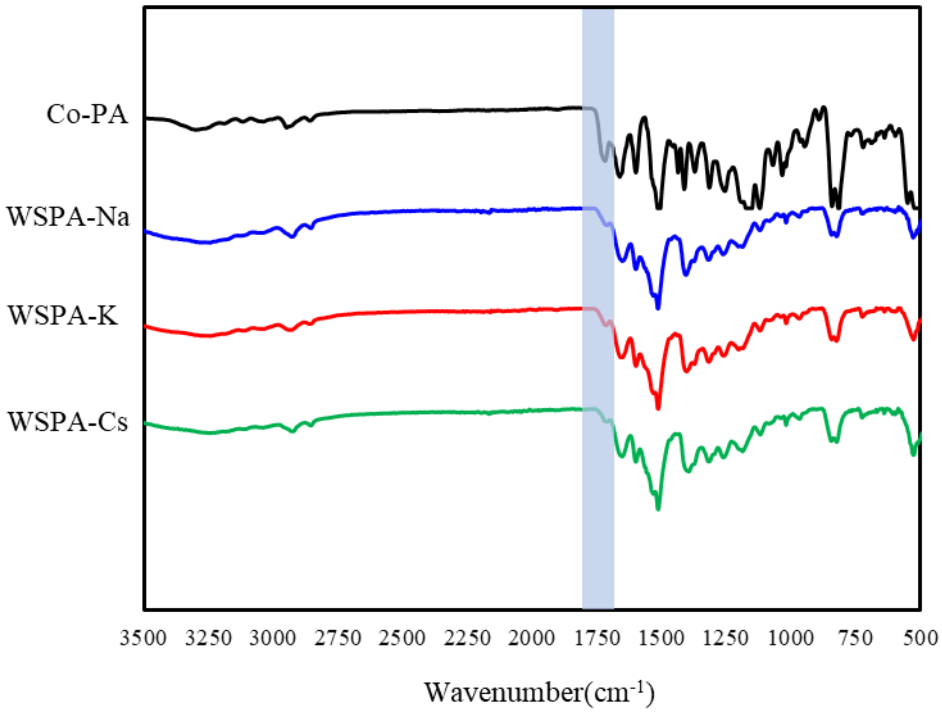

Figure 3-2. FT-IR spectra of WSPA films.

The 5% and 10% weight loss temperature (T_{d5}, T_{d10}) of the obtained WSPAs showed approximately 340 to 350 °C. These values were comparable to the original 4ACA-based *co*-polyamide.[11] On the other hand, T_g were not determined lower degradable temperature. In addition, optical properties such as the yellow index and transparency at 400 and 450 nm were nearly the same at values of *co*-polyamide. Figure 3-3,4 showed obtained WSPA films and transparency curves.

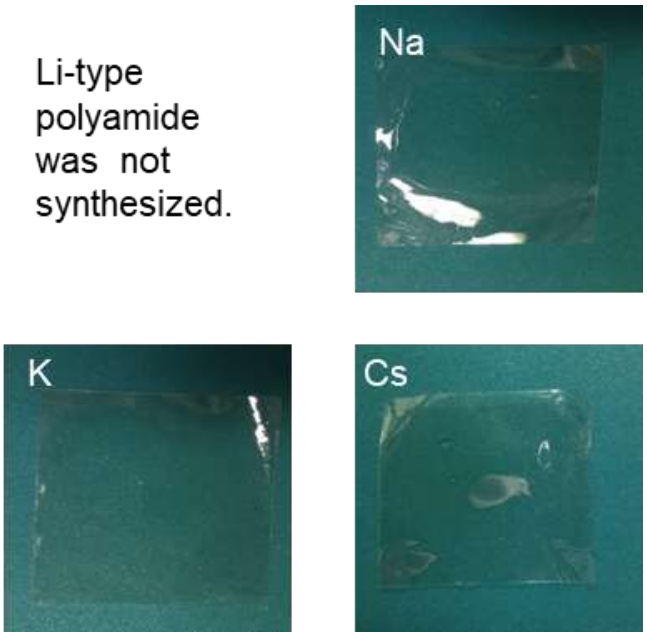

Figure 3-3. Photographs of obtained WSPA films.

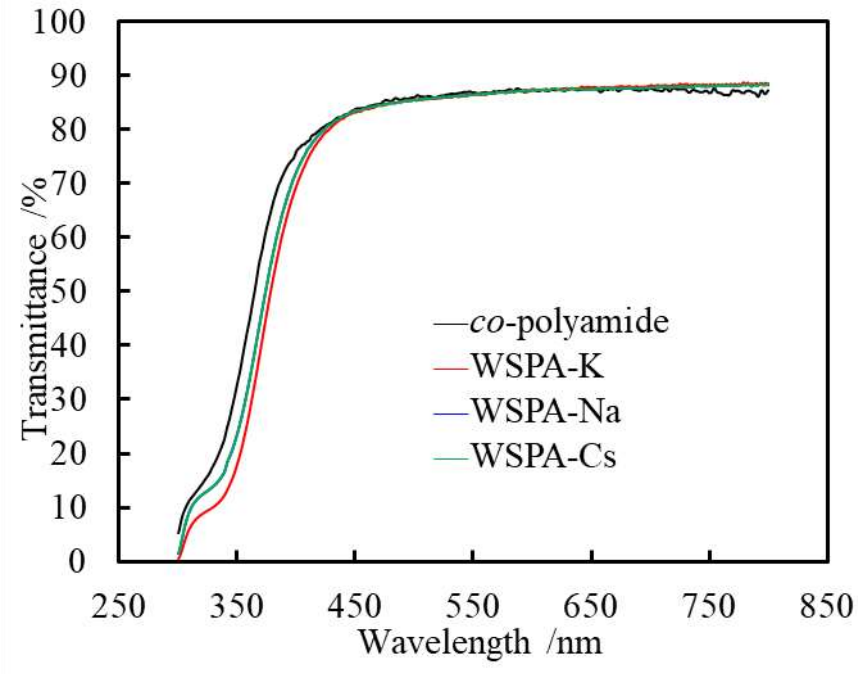

Figure 3-4. Transmittance spectra of WSPA films.

Furthermore, Mechanical properties were measured by tensile test. The stress-

strain curves were shown in Figure 3-5. As a result, Young's moduli were declined but strength and elongation at break were increased than *co*-polyamide. The results were suggested that electrostatic repulsion were working between polymer chains.

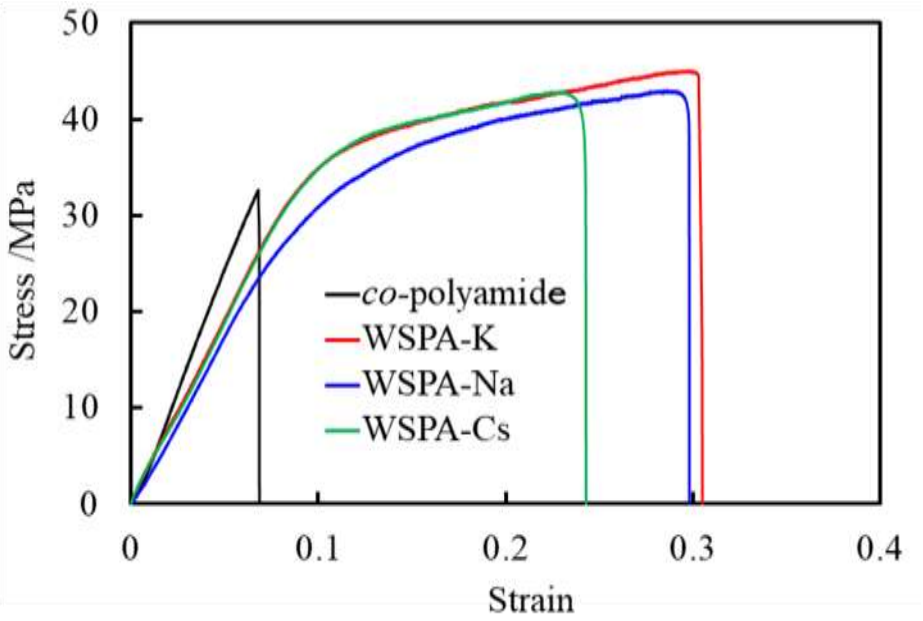

Figure 3-5. Stress-strain curves of WSPA films.

These results shown that the molding process can be performed with more volatile solvents such as water or methanol without degrading some properties. This resalts also indicates that the molding process can be performed with a lower environmental impact.

Insolubilized polyamides.

Water solubility means not only good processability but low water resistance.

Therefore, to use WSPAs in various environments, it is necessary to provide resistance to water and organic solvents (table 3-2).

Treated WSPA films aforementioned method, they were confirmed shrinking a little bit without collapsing or dissolution as shown Figure 3-6. The shrinkage is thought to be due to the crosslinking between carboxylate anions of polyamide side chains caused by divalent cations.

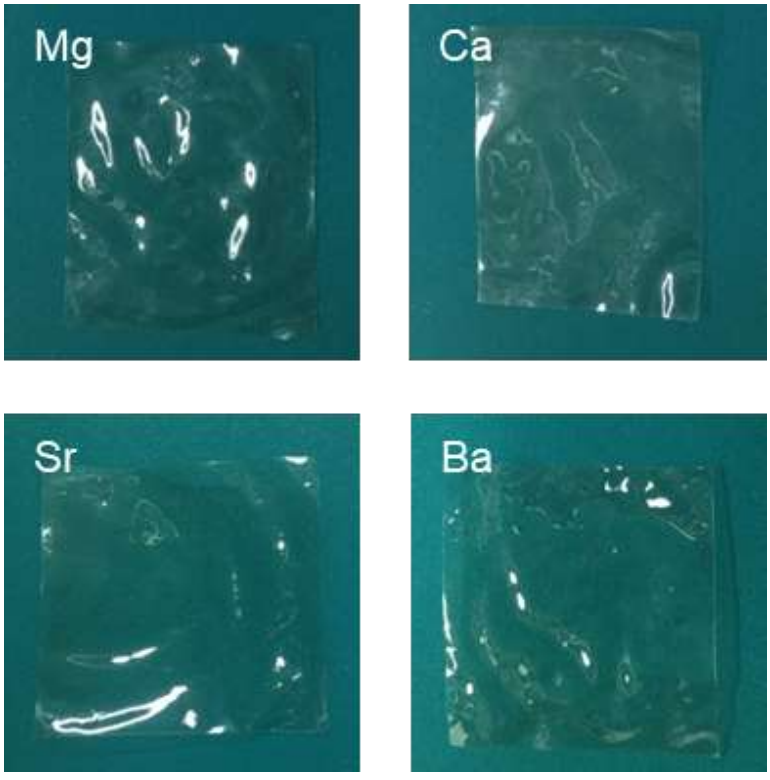

Figure 3-6. Photographs of obtained ISPA films.

Solubility tests for ISPAs were carried out by the same method for WSPAs. They

were not shown the solubility to pure water, H_2SO_4 or other typical organic solvents. Therefore, ISPA films were kept transparency at 400 nm and 450 nm (Figure 3-7). This is because the divalent cations as crosslinker did not absorb in the visible light range, as in addition, whitening was unlikely to occur due to the polyamide does not show crystalline under small strain.

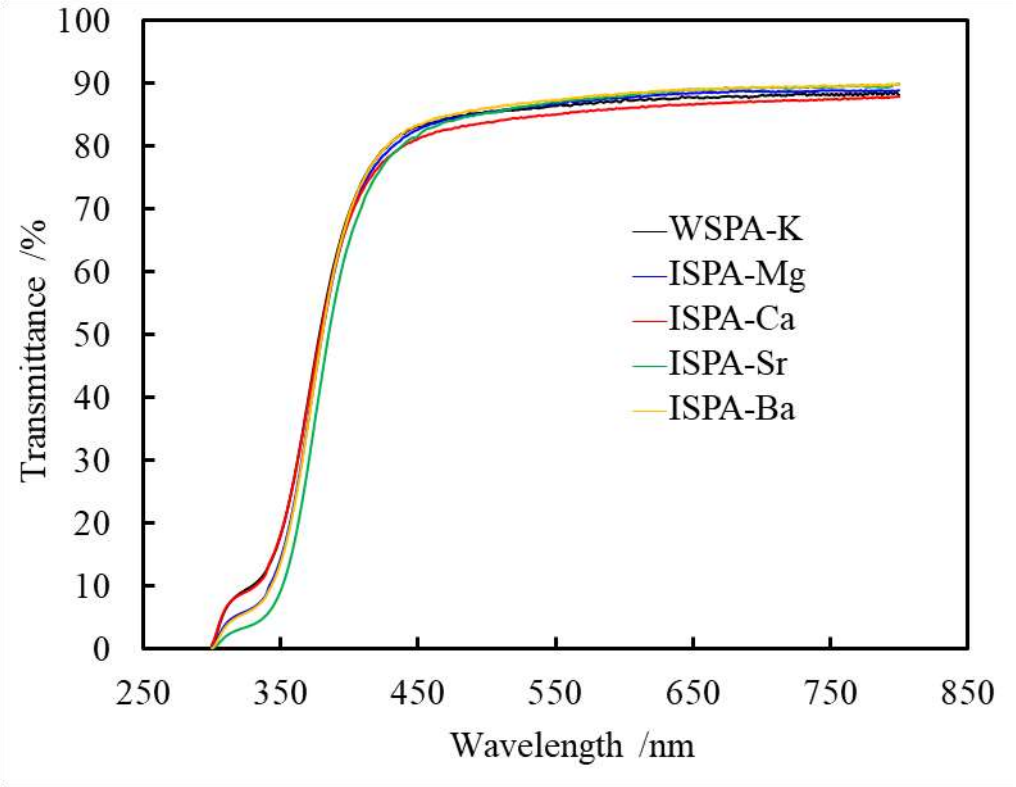

Figure 3-7. Transmittance spectra of ISPA films.

Table 3-2. Solubility of polyamide alkali earth metal salts.[a]

Type	Water	MeOH	EtOH	Hexane	THF	NMP	DMAc	DMF	DMSO	conc H_2SO_4
K	+	+	-	-	-	-	-	-	-	+
Mg	-	-	-	-	-	-	-	-	-	-
Ca	-	-	-	-	-	-	-	-	-	-
Sr	-	-	-	-	-	-	-	-	-	-
Ba	-	-	-	-	-	-	-	-	-	-

[a]Sample, 5 mg; solvent, 1.0 mL; solubility, + (soluble), − (insoluble).

In addition, thermal and mechanical properties were increased than WSPAs (Figure 3-8,9). For instance, T_{d5} and T_{d10} were increased about 30 °C than WSPA-K. Therefore, mechanical strengths and Young's moduli were greatly increased than WSPA-K. These results were shown that polymer chains were strongly cross-linked by multivalent cations. In addition, elongation at break of ISPA-Ba was higher than WSPA-K. In generally, there is a trend that the interaction between smaller metal cations and ligands works more strongly. Barium ion is the biggest cation in this study. For that reason, high elongation was expressed due to the recuring scission and recombination when the films were stretched.

These polyamide properties were shown in Table 3-3.

Polyamide salts did not show any glass transition temperatures. This may be due to the glass transition temperature being higher than the decomposition initiation temperature, as reported for other ionomers.[19,20]

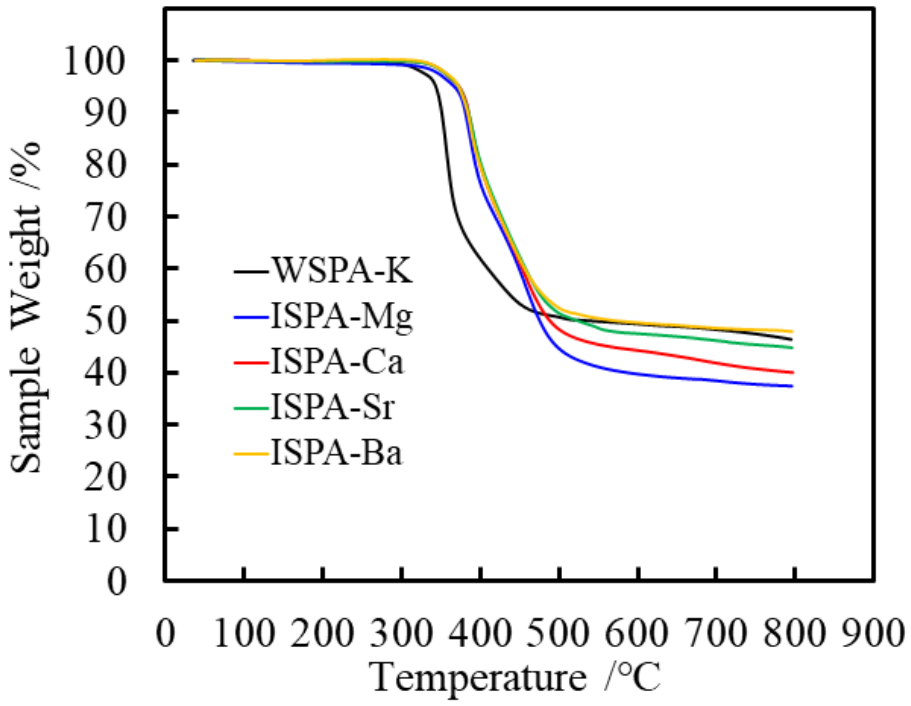

Figure 3-8. TGA curves of ISPAs.

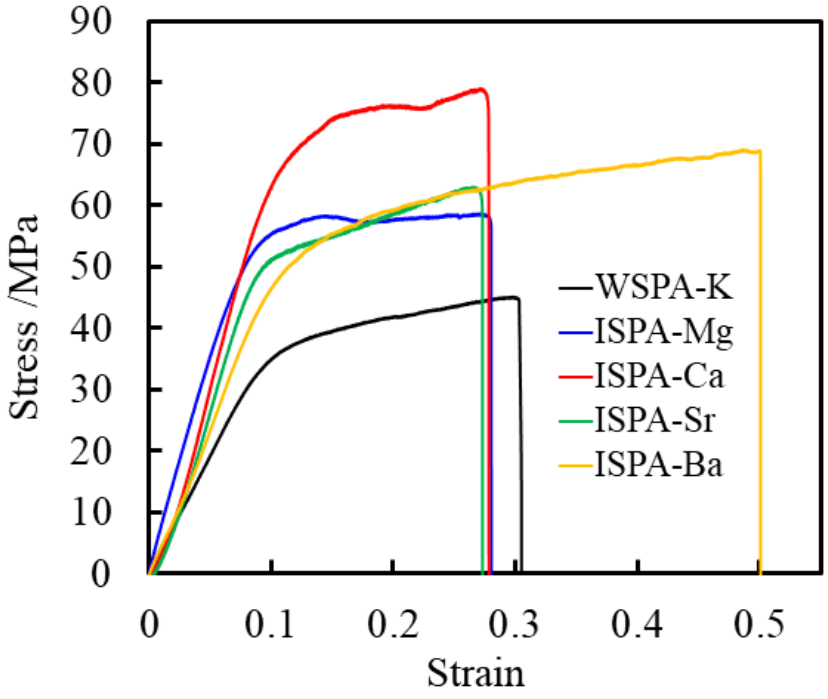

Figure 3-9. Stress-strain curves of ISPA films.

Table 3-3. Properties of polyamide salts.[a]

type	σ(MPa)[b]	E(MPa)[b]	ε(mm/mm)[b]	U_d(J/m^3)[b]	T_g[c]	T_{d1}[d]	T_{d5}[d]	T_{d10}[d]	*Transparency (%)*[e]		YI[f]
									400 nm	450 nm	
Me	36.8 ± 4.6	480 ± 38	0.104 ± 0.017	2 ± 1	191	302	337	350	75.9	83.7	3.04
Na	41.3 ± 6.1	371 ± 31	0.296 ± 0.078	10 ± 3	NO	209	340	358	72.1	83.5	3.2
K	41.0 ± 4.4	359 ± 22	0.359 ± 0.069	12 ± 7	NO	308	343	351	69.6	83.2	3.18
Cs	45.4 ± 6.6	376 ± 38	0.310 ± 0.033	10 ± 2	NO	295	338	347	72.2	83.5	2.96
Mg	55.5 ± 2.5	615 ± 48	0.199 ± 0.052	12 ± 3	NO	315	367	381	68.7	81.2	7.31
Ca	79.6 ± 2.3	703 ± 20	0.256 ± 0.042	15 ± 3	NO	341	373	385	68.4	81.2	7.22
Sr	62.5 ± 5.1	566 ± 59	0.248 ± 0.047	12 ± 3	NO	340	372	385	64.8	81.6	7.41
Ba	69.5 ± 4.1	459 ± 40	0.536 ± 0.051	29 ± 7	NO	342	372	384	69.3	83.4	6.69

[a]All materials were measured as films. [b]Mechanical properties, E, σ, ε, and U_d were measured by tensile tests at 0.50 mm min^{-1} of tension rate.

[c]Measured by DSC; heating rate, of 10 °C min^{-1}; N_2 atmosphere. [d]Measured by TGA; heating rate, of 5 °C min^{-1}; N_2 atmosphere.

[e]Yellow Index and transparency at 400 nm and 450 nm were measured by spectrophotometry.

CNF/WSPA composite films

Granted water solubility to polyamide would also facilitate mixing with water-based fillers such as CNF. In this study, CNF/WSPA composite films were prepared in various ratios. Prepared films and transparency were shown in Figure 3-10,11. Prepared films in this study showed high transparent these values were not far behind from pure WSPA-K film. In generally, when materials of different refractive indexes, they turn opaque even if they are transparent. However, composite films including low concentration CNF (0.5, 1%) showed high transparency. This resalt suggests that the CNF have been dispersed into WSPA-K to a size below wavelengths of visible light.

FT-IR spectra of CNF/WSPA-K composite films were shown in Figure 3-12. The spectra of composite films showed a peak assigned to the ether bond of CNF, 1000 cm^{-1} (C-O stretching). The results confirm that WSPA-K and CNF are indeed mixed.

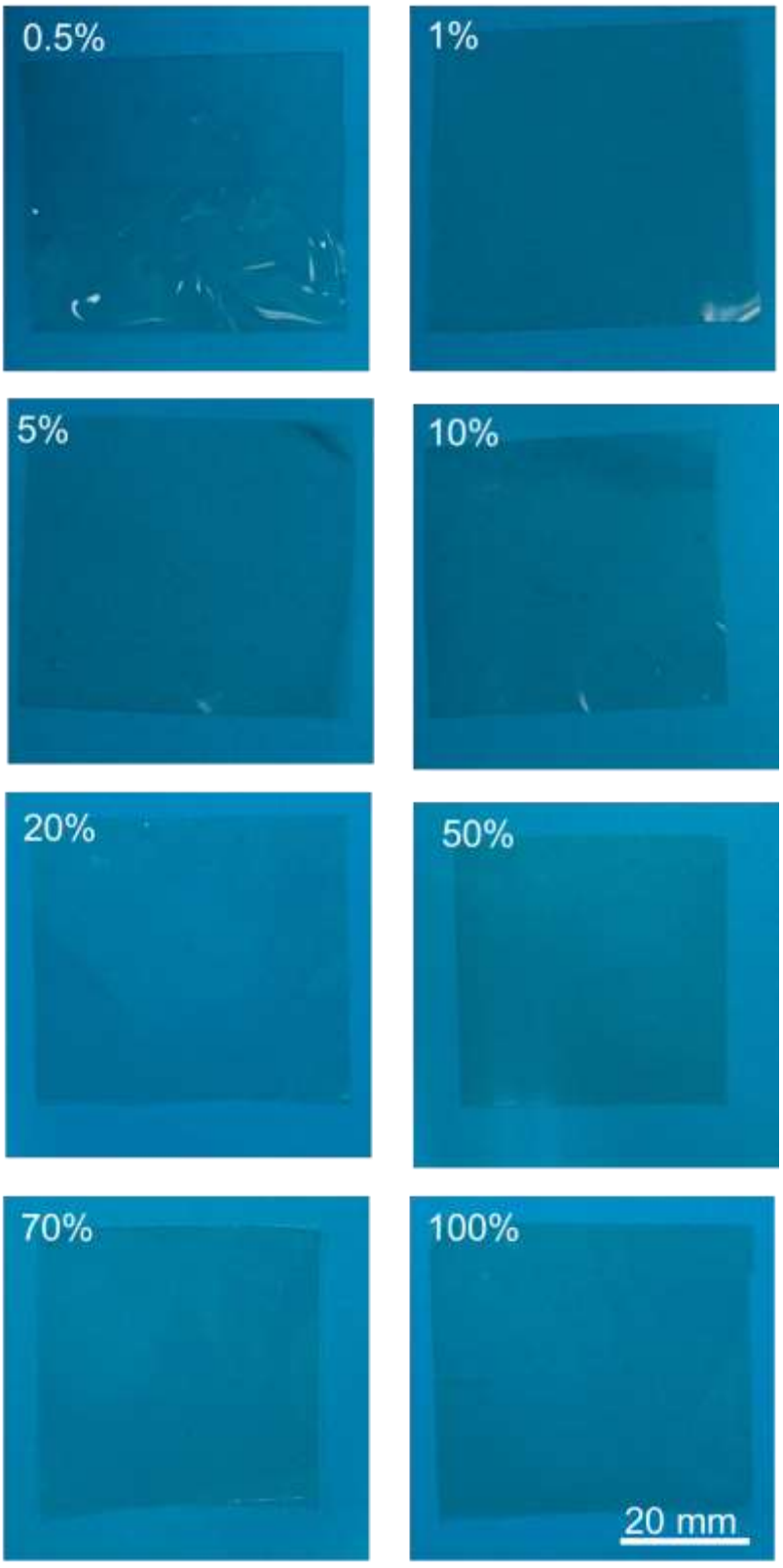

Figure 3-10. Photographs of obtained CNF/WSPA-K composite films.

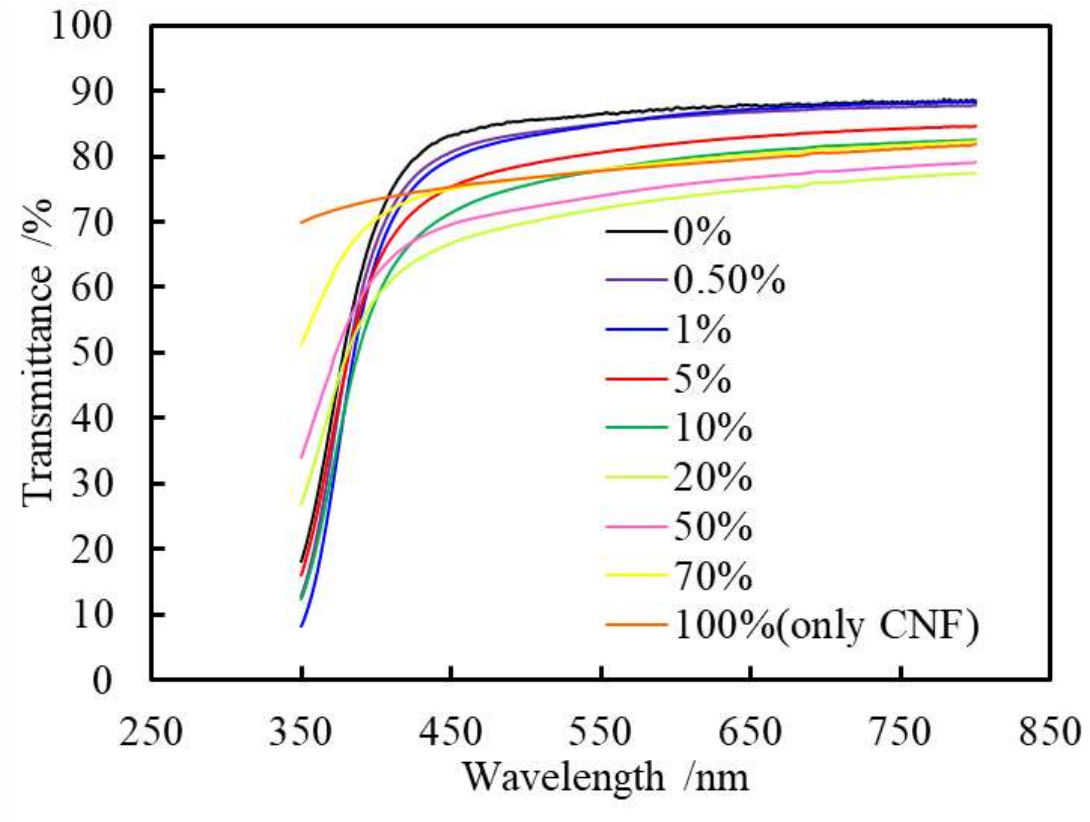

Figure 3-11. Transmittance spectra of CNF/WSPA-K composite films.

The POM images were shown in Figure 3-13. Observation of the figure 3-13 showed that coarse, rod-like agglomerates were dispersed in the film with high CNF content. The decrease in transparency is thought to be due to these agglomerates.

On the other hand, mechanical properties of composite films were improved from WSPA film as shown in Figure 3-14 and Table 3-4. In particular, the 0.5-10% CNF films also showed increased strain and toughness. This is thought to be due to rigidity of CNF and the interaction between the hydroxyl groups in CNF and acetoamido group in the side chains of polyamide.

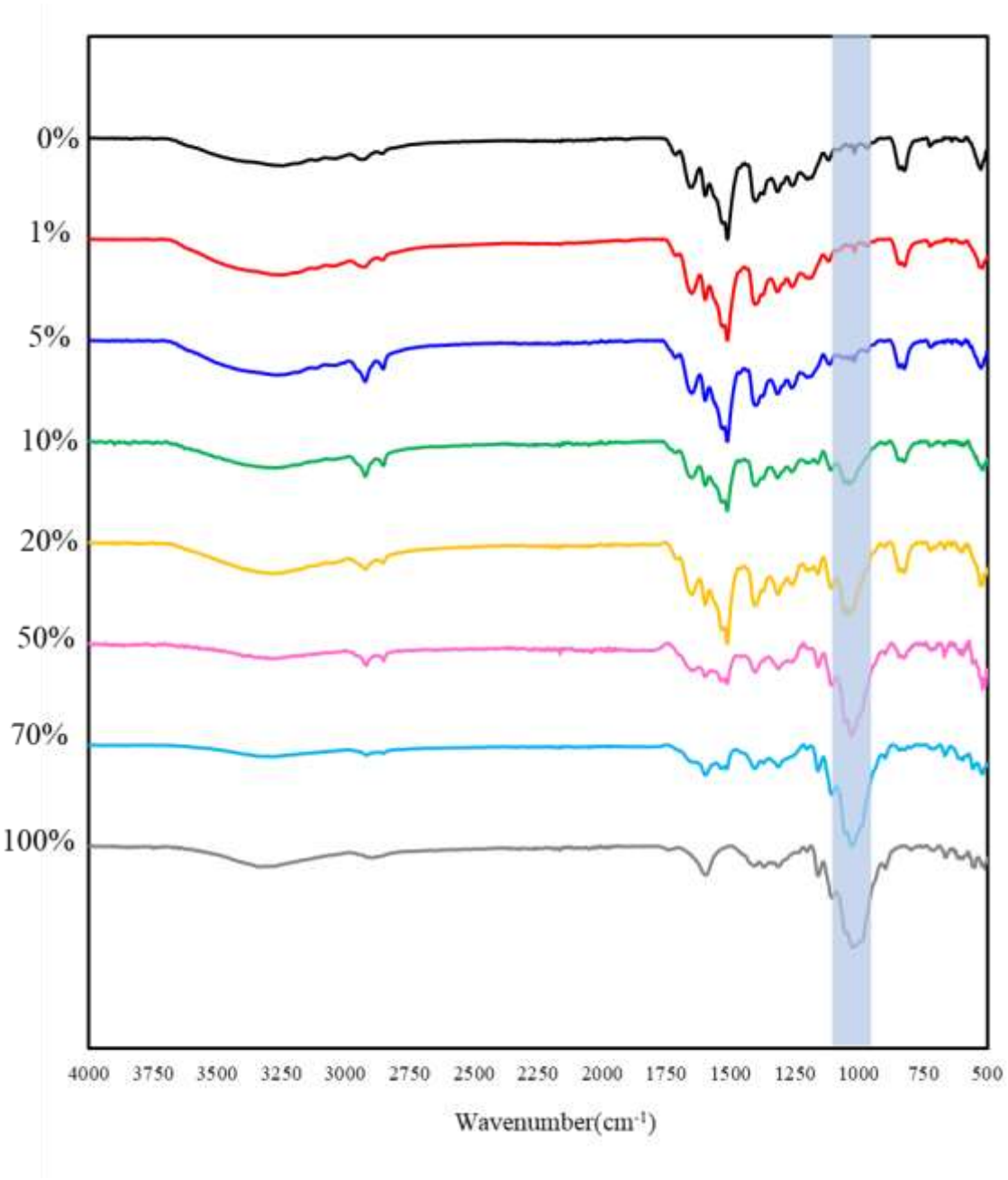

Figure 3-12. FT-IR spectra of CNF/WSPA-K composite films.

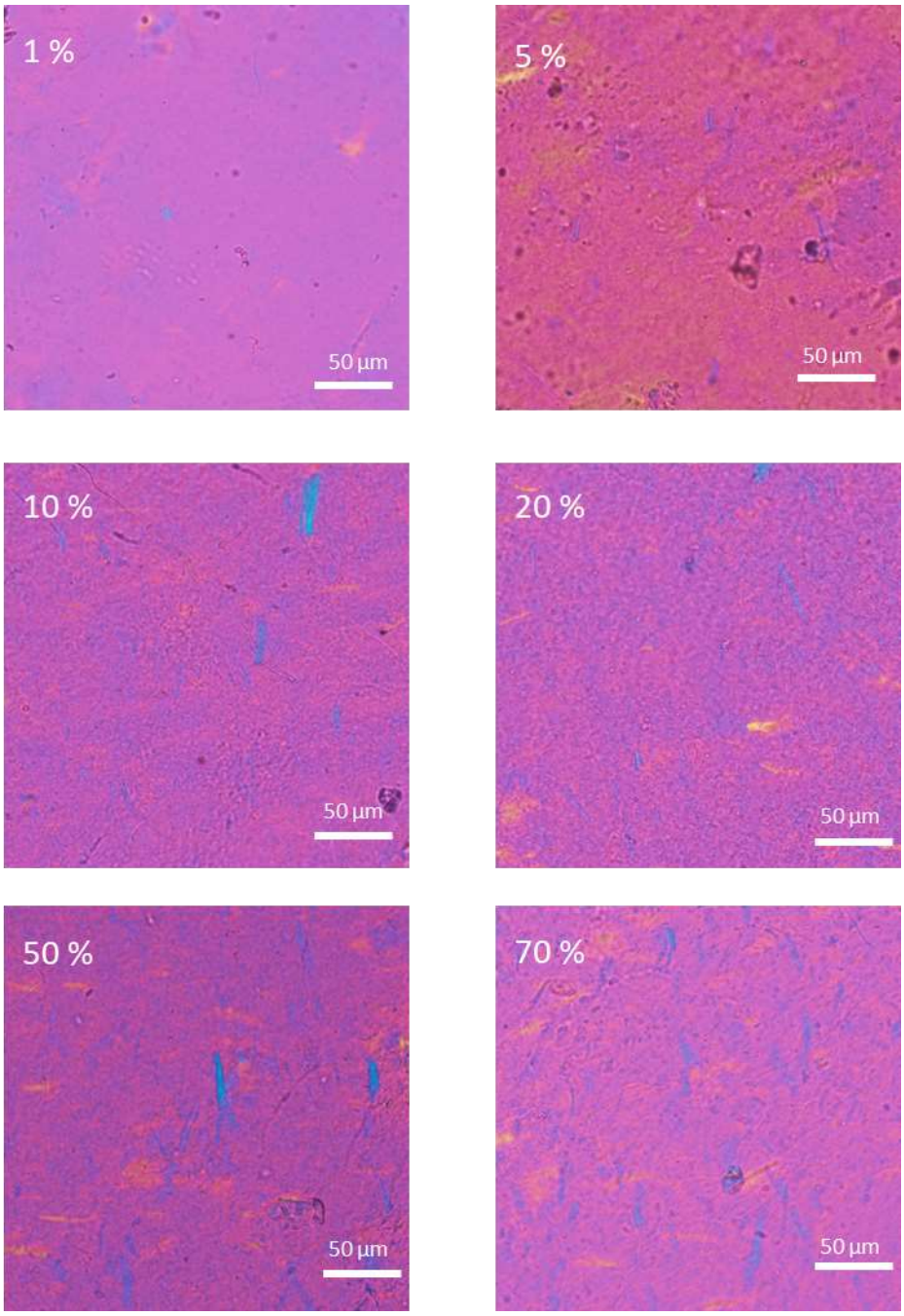

Figure 3-13. POM images of CNF/WSPA-K composites films.

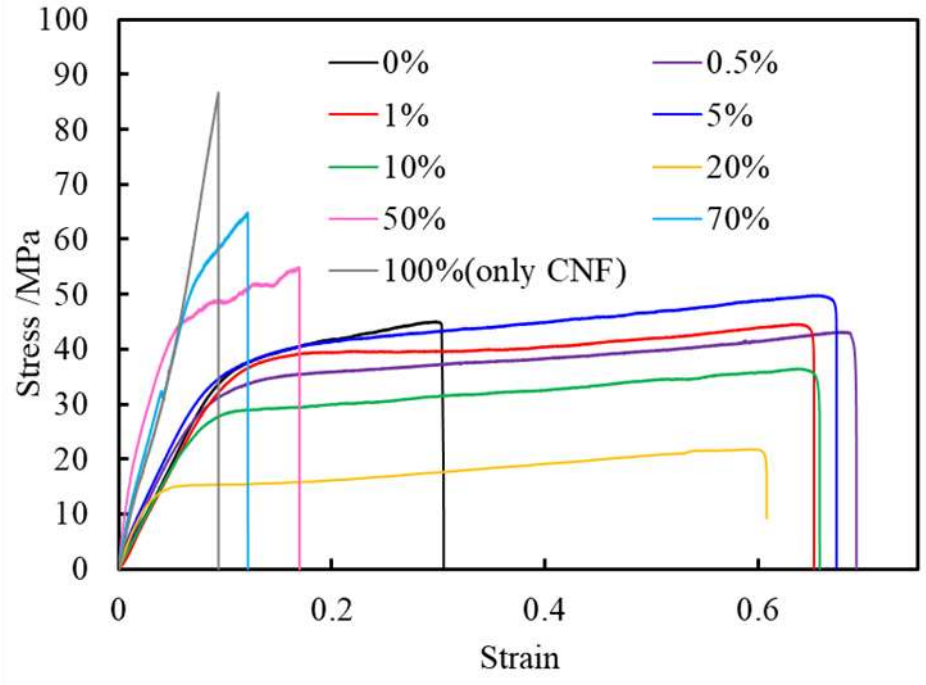

Figure 3-14. Stress-strain curves of CNF/WSPA-K composite films.

Table 3-4. mechanical properties of CNF/WSPA-K composite films.[a]

CNF ratio (%)	Strength (MPa)	Young's modulus (MPa)	Strain at break (mm/mm)	Strain energy density (J/m^3)
0	41.0 ± 4.4	359 ± 22	0.359 ± 0.069	12 ± 7
0.5	44.9 ± 5.0	449 ± 68	0.666 ± 0.227	25 ± 11
1	42.8 ± 2.5	426 ± 106	0.633 ± 0.212	23 ± 8
5	48.2 ± 3.0	442 ± 93	0.665 ± 0.171	26 ± 8
10	36.4 ± 2.8	355 ± 86	0.565 ± 0.166	18 ± 6
20	24.6 ± 4.8	752 ± 147	0.438 ± 0.104	7.4 ± 1.8
50	54.5 ± 2.7	1254 ± 255	0.139 ± 0.019	6.2 ± 0.87
70	35.8 ± 6.1	1300 ± 416	0.039 ± 0.009	0.59 ± 0.44
100	78.6 ± 25.2	793 ± 89	0.084 ± 0.008	3 ± 1

[a]Mechanical properties, E, σ, ε, and U_d were measured by tensile tests at 0.50 mm min^{-1} of tension rate.

On the other hand, composite films containing higher concentrations of CNF showed reduced elongation and were stiffer films. This may reflect the rigidity of CNF, but

also the loss of flexibility due to agglomerates that behaved as defects, as identified in Figure 3-13.

In addition, TEM observations were made (Figure 3-15). The figure shows a linear region of several micrometers (Figure 3-15A) and dispersed fibers of several dime nanometers (Figure 3-15B), respectively.

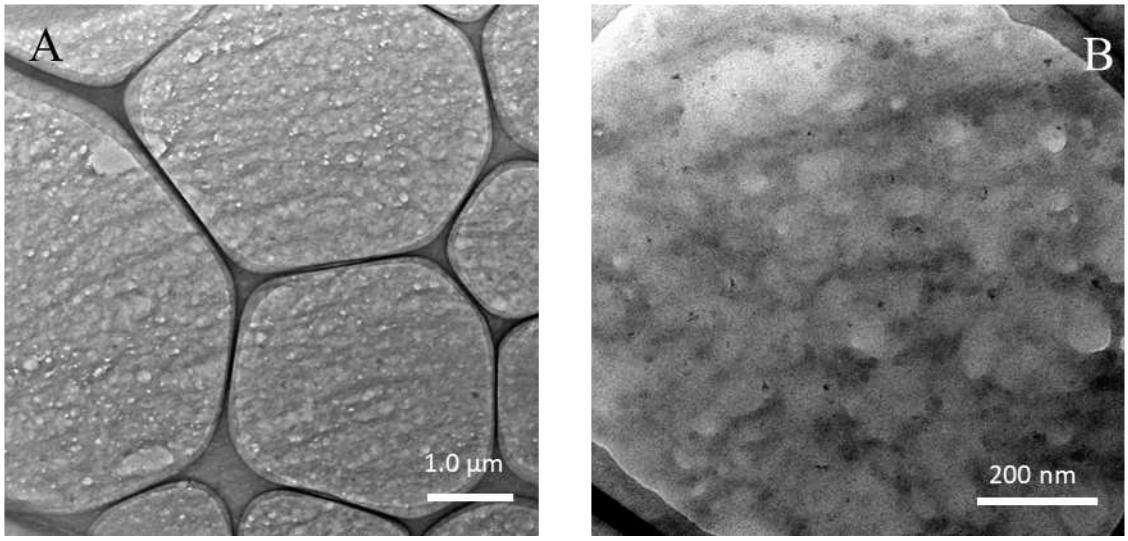

Figure 3-15. TEM images taken at two different magnifications of 50% CNF/WSPA film.

3.4 Conclusion

4-amino cinnamic acid-based polyamide metal salts were synthesized by the action of alkali metal hydroxides on polyamide. The polyamides were soluble in water or methanol. The crosslinked structure was introduced by the action of alkaline earth metal ions on this water-soluble polyamide. The polyamide was then cross-linked with alkaline earth metal ions, which gave the polyamide high chemical stability and solubility not only in water and methanol, but also in common organic solvents and strong acids. In addition, the polyamide has improved heat resistance and mechanical properties, and the barium salt in particular has greatly improved toughness.

Furthermore, composite films were prepared by dispersing cellulose nanofibers, a water-soluble filler, in the synthesized water-soluble polyamide. The resulting films not only had high transparency, but also showed improved mechanical properties. This is thought to be due to the interaction between the hydroxyl groups of the cellulose nanofibers and the amide moieties of the polyamide.

These results indicate that polyamide can not only be molded and processed more safely, but also its properties can be controlled by adding metal ions and water-soluble fillers.

REFERENCES

1. Lim,J.,G., Gupta, B., S., George, W.,The potential for high performance fiber from nylon 6. *Prog. Polym. Sci*, **1989**, *14*, 763-809.

2. Pan, G., Zhao, Y., Xu, H., Hou, X., Yang, Y., Compression molded composites from discarded nylon 6/nylon6,6 carpets for sustainable industries, *J. Clean*. **2016**, *117*, 212-220

3. Ali, A., M., The impact of processing conditions on the structural and optical properties of the as-spun polyamides fibers *Microsc. Res. Tech.*, **2019**,*82*, 1922-1927.

4. Basavaraj, E., Siddaramaiah, B., R., A study on mechanical, thermal, and wear characteristics of nylon 66/molybdenum disulfide composites reinforced with glass fibers, Polymer Composites, **2012**, *33*, 1570-1577.

5. Bera, D., Chatterjee, R., Banerjee, S., Aromatic polyamide nonporous membranes for gas separation application *e-Polymers*, **2021**, *21*,108–130

6. Morgan, R., J., Butler, N., L., Hydrolytic degradation mechanism of Kevlar 49 fibers when dissolved in sulfuric acid *Polymer Bulletin* **1992** ,*27*, 689-696.

7. Takada, K., Mae, Y., Kaneko, T., Fluorinated and Bio-Based Polyamides with High Transparencies and Low Yellowness Index. Polymers 2018, 10, 1311.

8. Kawasaki, Y., Aniruddha, N., Minakawa, H., Masuo, S., Kaneko, T., Takaya, N., Novel poly-condensed biopolyamide gen-erated from biomass-derived 4-aminohydrocinnamic

acid. Appl. Microbiol. Biotechnol. 2018, 102(2), 631-639.

9. Tateyama, S., Masuo, S., Suvannasara, P., Oka, Y., Miyazato, A., Yasaki, K., Teerawatananond, T., Muangsin, N., Zhou, S., Ka-wasaki, Y., Zhu, L., Zhou, Z., Takaya, N., Kaneko, T., Ultra-strong, transparent polytruxillamides derived from microbial photodimers. Macromolecules 2016, 49(9), 3336-3342.

10. Shin, H., Tateyama, S., Kaneko T., Synthesis of Photo-degradable Polyamide Rotaxanes with Cinnamate Photodimer and Cyclodextrin. J Mater. Life Soc. 2014 26(2), 25-31.

11. Funahashi, Y., Yoshinaka, Y., Takada, K., Kaneko, T., Self-standing Nanomembranes of Super-Tough Plastics. *Langmuir* **2021**, *38, 17*, 5128-5134.

12. Peng, X., Zhang, Z., Improvement of paint adhesion of environmentally friendly paint film on wood surface by plasma treatment, *Progress in Organic Coatings*, **2019**, *134*, 255

13. Sun, Q., Schork, F., J., Deng, Y., Water-based polymer/clay nanocomposite suspension for improving water and moisture barrier in coating *Compos. Sci. Technol.*, **2007**, *67*, 1823-1829.

14. Jia, L., Zhou, C., Sun, W., Xu, L., Yan, D., Li, Z., Water-based conductive ink for highly efficient electromagnetic interference shielding coating, *Chem. Eng. J.*, **2020**, *384*, 123368.

15. Saito, T., Kimura, S., Nishiyama, Y., Isogai, A., Cellulose Nanofibers Prepared by

TEMPO-Mediated Oxidation of Native Cellulose *Biomacromolecules*, **2007**, *8*, 2485-2491.

16. Isogai, A., Saito, T., Fukuzumi, H., TEMPO-oxidized cellulose nanofibers *Nanoscale*, **2011**, *3*, 71-85

17. Noguchi, T., Niihara, K., Kurashima, A., Iwamoto, R., Miura, T., Koyama., A., Endo, M., Marubayashi., H., Kumagai., A., Jinnai, H., Isogai, A., Cellulose nanofiber-reinforced rubber composites prepared byTEMPO-functionalization and elastic kneading., *Compos. Sci. Technol.,* **2021,** *210*, 108815.

18. Kim, H., Roy, S., Rhim, J., Effects of various types of cellulose nanofibers on the physical properties of the CNF-based films *J. Environ. Chem. Eng.*, **2021**, *9*,106043.

19. Kim, S.; Kim, J., Relationships between the Glass Transition Temperatures and the Type of Cations in Poly(ethyl acrylate) Ionomers, *Macromolecules,* **2003**, *36*, 2382-2386.

20. Wu, Q.; Weiss, R.A., Viscoelastic properties of poly(styrene-*co*-vinylphosphonate) ionomers, *Polymer* ,**2007**, *48*,7558-7566.

Chapter 4. Compositing with nano-fillers

4.1 Introduction and research background

Compared to inorganic glass, transparent polymer materials are lighter, more flexible, and easier to mold and process, and are attracting attention in the photonics field, where microfabrication is required, as well as in flexible devices and other applications. In order to apply polymer materials in a wide range of fields, it is necessary not only to have high transparency but also to enhance properties such as mechanical strength, heat resistance, and chemical stability.[1-7]

In addition to transparency, it is also important to control the refractive index. However, in general, organic materials have a narrower range of refractive indices than inorganic materials due to the fewer types of constituent elements, and it is difficult to control the refractive indices. Since it is particularly difficult to achieve a high refractive index, methods to control the refractive index by hybridization with inorganic materials having a high refractive index have been reported.

In this study, I focused on sol-gel reaction as a preparation method for organic-inorganic composite materials.[8-12]

The sol-gel reaction is characterized by its high uniformity because it can be prepared from a solution state.[13-16] However, the alkoxides used as raw materials for titanium dioxide and zirconium oxide, which contribute to high refractive index, are highly

reactive, and it is necessary to devise a way to disperse them without affecting transparency.

Therefore, the objective of this chapter is to prepare composite materials with high heat resistance and high refractive index using the alcohol-soluble polyamide described in the previous chapter as a matrix.

4.2 Experimental

4.2.1 Materials

Methanol (99.8%), 2-propanol (99.7%), 1-butanol and ammonia solution (28.0%) were purchased from Kanto Chemical Co., Inc. Titanium tetraisopropoxide, Titanium tetrabutoxide, 85% Zirconium butoxide and 1-butanol solution were purchased from Wako Pure Chemical Industries. COOK type 4-aminocinnamic acid-based *co*-polyamide (WSPA-K) as matrix was synthesized by the method described in the previous chapter.

4.2.2 Preparation of polyamide/metal oxide nanocomposites

Membrane preparation

polyamide/metal oxide nanocomposites were prepared by sol-gel method

(scheme 4-1). The reaction of 10% titania/ polyamide procedures was follows. 18.0 mg WSPA-K was dissolved in 1.8 mL of methanol, and then 51 μL of ammonia solution as catalyst was added to polyamide solution. Moreover, titanium tetraisopropoxide 2-propenol solution were 7.11 mg of titanium tetraisopropoxide, the weight set to get 2 mg after reaction (here, when butoxide was used as the raw material, butanol was used as the solvent.), in dissolved 0.3 mL of 2-propanol was added dropwise into the above solution and then stirred at room temperature for 30 min. After that, the membrane formed on glass plate by spin-coating method, and dried at room temperature for 12h, 60°C for 2h, 100°C for 2h and 150°C for 2h.

Film preparation

The preparation of composite films procedures was follows. The mixed solution of polyamide and metal alkoxide was poured into a petri dish. After that, the petri dish was dried by stood for 3 weeks at room temperature with the lid on. After the solvent was sufficiently volatilized, the film was peeled off from petri dish and heat-dried in the same steps as above.

Scheme 4-1 syntheses of polyamide/metal oxide nanocomposites.

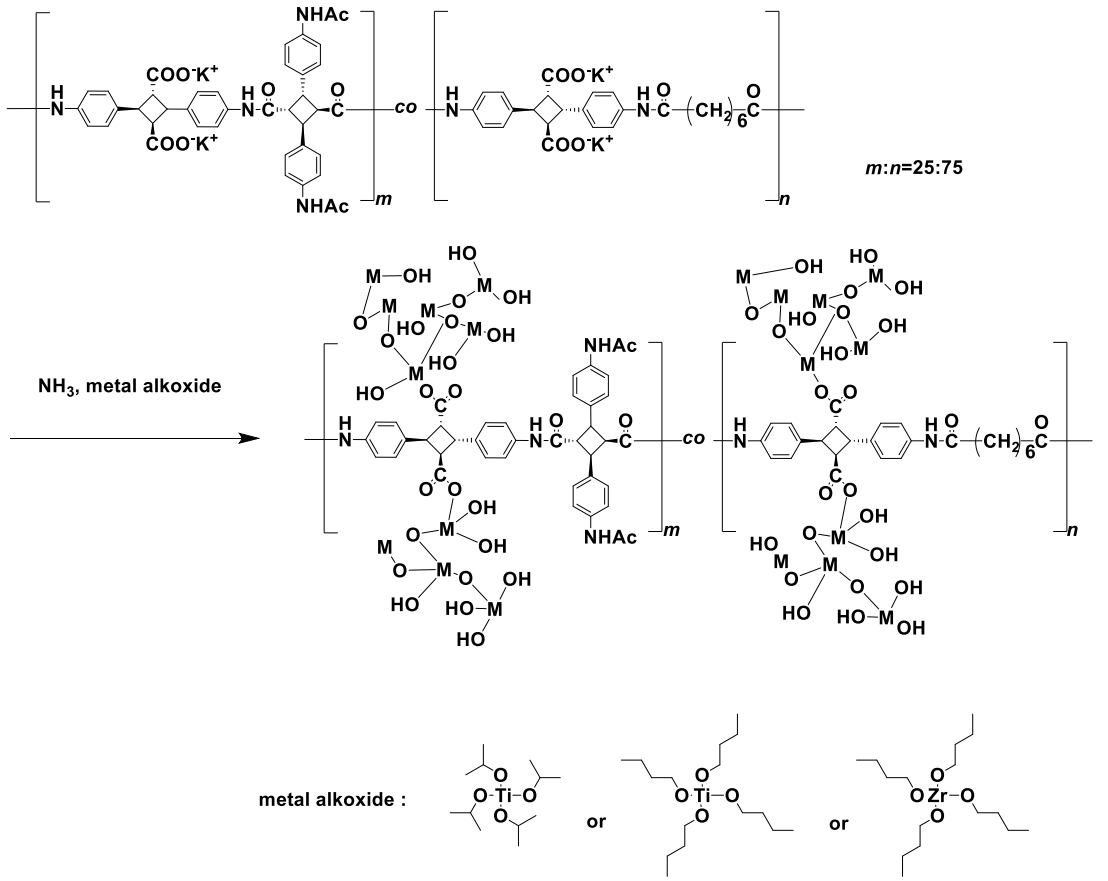

4.2.3 Characterization of polyamide/metal oxide nanocomposites

Ultraviolet-Visible Absorption Spectroscopy (UV-Vis) was performed by V-670 (JASCO) in 250 nm to 800 nm as measured range. Refractive indexes and thickness of nano-membranes which were adhered on glass plates were measured by using an optical thickness meter (Otsuka Electronics). Thermal gravimetrical analysis (TGA) was carried out by STA 7200 (HITACHI) under nitrogen flow (flow rate, 200mL min^{-1}) from 25 °C to 800 °C at heating rate of 5 °C min^{-1}. Fourier transform infrared spectroscopy (FT-IR) measurement was carried out using Spectrum 100 and Spectrum Spotlight 200 (Perkin Elmer) by

Attenuated Total Reflection method. X-ray diffraction (XRD) measurements was performed by using Smart Lab (Rigaku). The obtained samples were observed by Transmission Electron Microscope (TEM) H-7650 (HITACHI).

4.3 Results and discussion

Firstly, the refractive index measurements of polyamide metal salts in the previous chapter are shown in Figure 4-1.

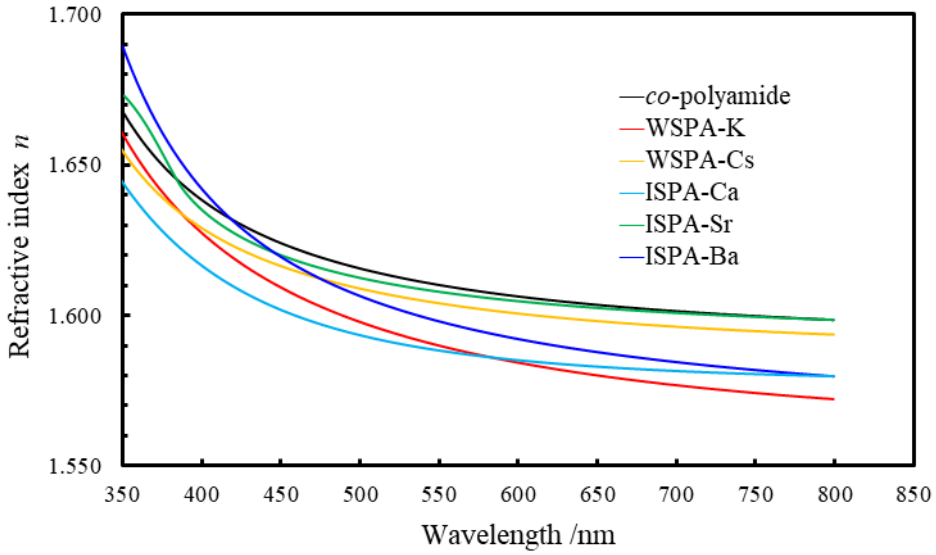

Figure 4-1. Refractive index curves of polyamides.

The refractive index of the polyamides did not change significantly, although there were differences depending on the structure of the side chains.

The lower refractive index of the metal salt than that of the polyamide before the

reaction was probably due to the water content of membranes.

The metal alkoxides used in this chapter are known to be relatively stable in alcohols.

Therefore, WSPA, which has solubility in methanol, is considered appropriate as a matrix. As in the previous chapter, WSPA-K was used as the matrix of the composites.

In order to verify the difference in refractive index due to the type of element, membranes of TiO_2 and ZrO_2 complexed in the same ratio (8.1 vol%) used for titanium butoxide and zirconium butoxide as the raw materials were prepared and the refractive indexes were measured. The results are shown in the Figure4-2. The vol% values were calculated using the density of amorphous TiO_2 as 3.80 and amorphous ZrO_2 as 5.85.[17,18]

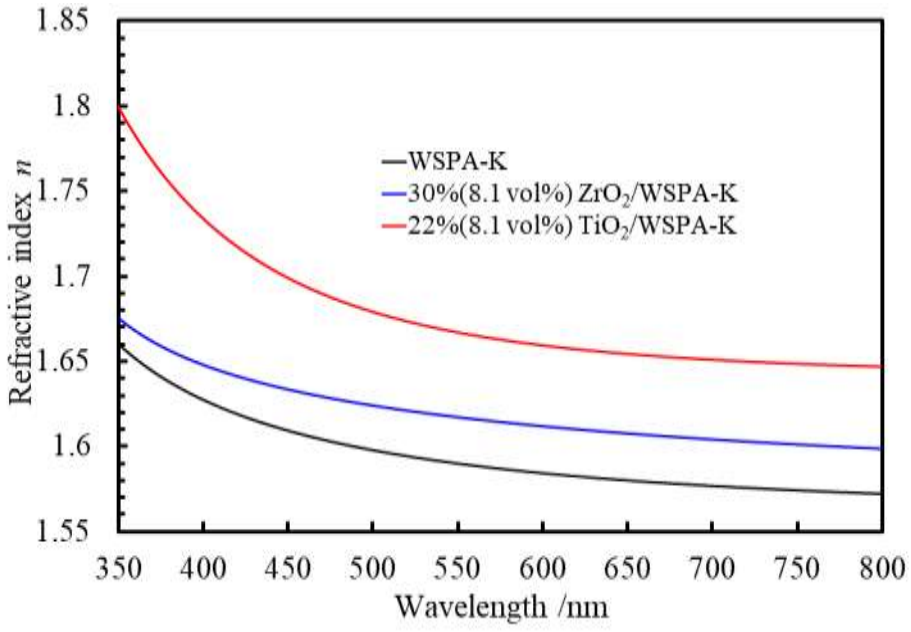

Figure 4-2. Refractive index curves of metal oxide/WSPA-K composite membranes.

The refractive index was improved for both titanium dioxide and zirconium oxide.

As is clear from the above results, the refractive index was higher for the membrane composited with titanium oxide than for the thin film containing zirconium oxide. This result was consistent with the generally known pecking order of refractive indices of oxides.

Secondly, the difference in refractive index between different titanium dioxide raw materials was examined. The results are shown in Figure 4-3.

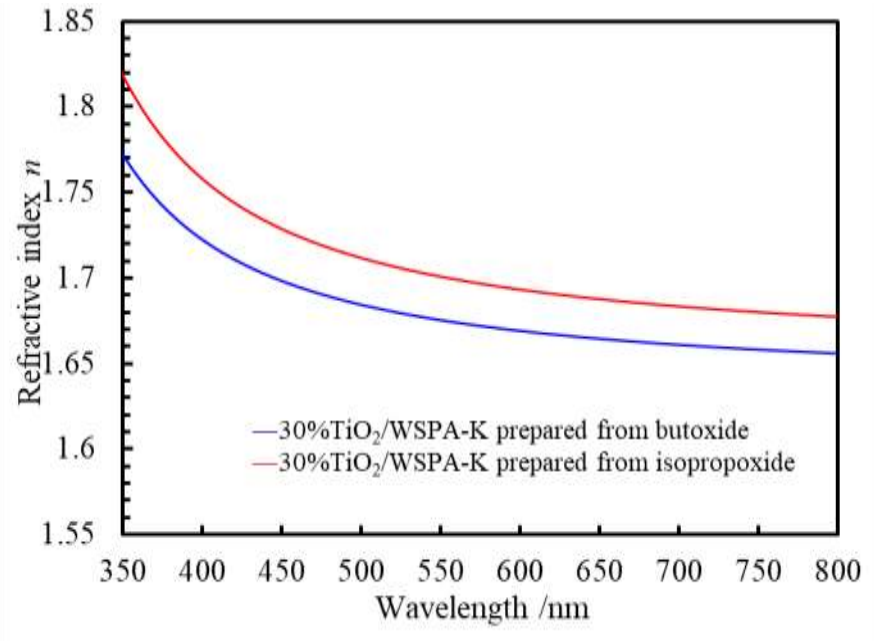

Figure 4-3. Refractive index curves of titanium oxide/WSPA-K composite membranes prepared from two types of raw materials.

As is clear from the Figure 4-2, the composite film using titanium tetraisopropoxide as the raw material exhibited a higher refractive index than that of titanium tetrabutoxide.

This can be attributed to the difference in reactivity of the alkoxides used as raw materials and their compatibility with methanol and matrix.

In addition, to verify the difference in refractive index as a function of reaction time, membranes were formed after two types of agitation, one for 30 minutes and the other for 2 days, respectively, and the refractive indexes were measured. The measurement results are shown in Figure 4-4.

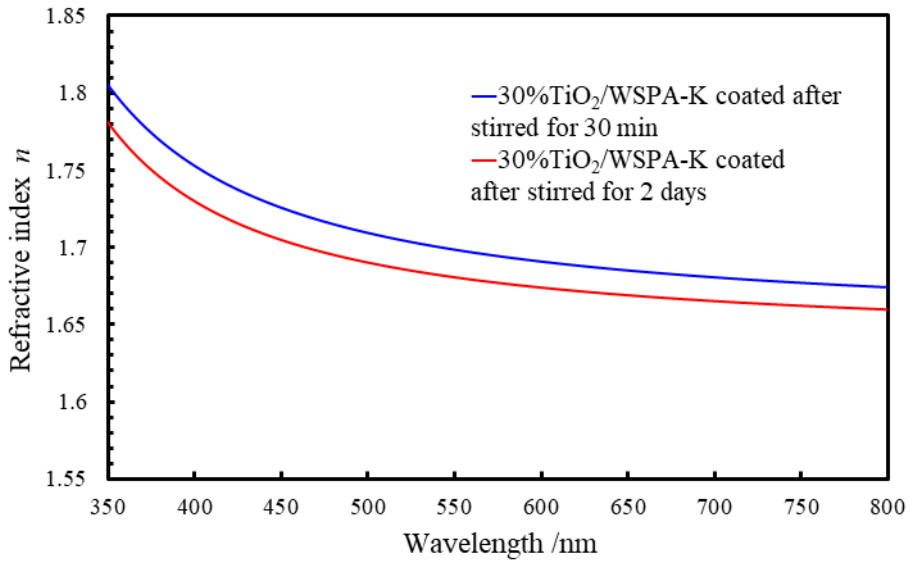

Figure 4-4. Refractive index curves of titanium oxide/WSPA-K composite membranes prepared any stirred time.

As shown in the Figure 4-3, the refractive index was higher when the stirring time was shorter. This is believed to be because the particles were coarsened by prolonged agitation and did not disperse sufficiently to affect the refractive index improvement.

Based on these results, composite films with different ratios of titanium

isopropoxide as raw material were prepared and their refractive indices were measured.

The resalts were shown in Figure 4-5.

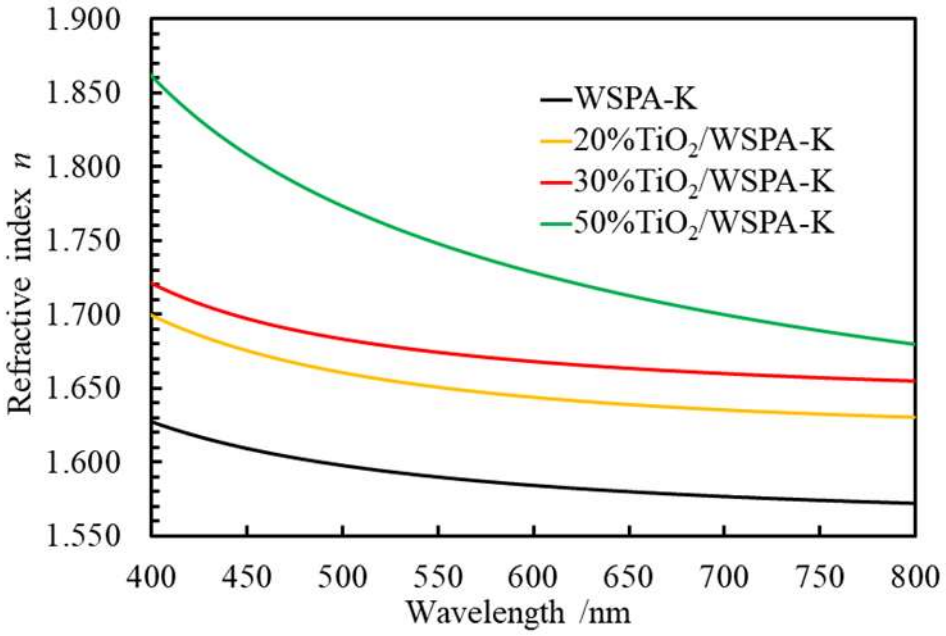

Figure 4-5. Refractive index curves of titanium oxide/WSPA-K composite membranes with various ratio.

As shown in the figure 4-4, the refractive index enhanced as the ratio of titanium dioxide in composite membranes increased.

In addition, composite films (containing TiO_2 10%,20%,30% and 40%) were prepared (Figure 4-6).

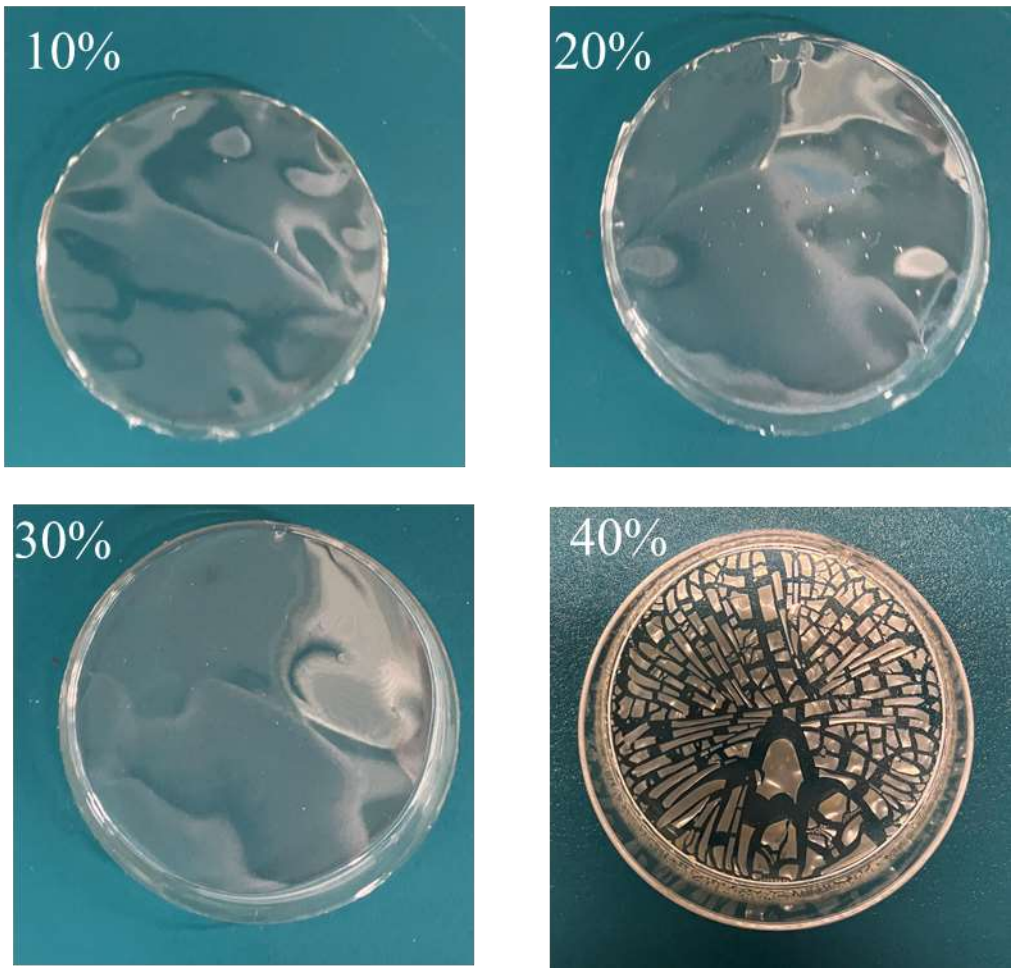

Figure 4-6. Obtained TiO_2/WSPA-K composite films.

Films were successfully obtained at 10%, 20% and 30%. On the other hand, the film was not obtained at 40% because of clacking. However, obtained films showed flexibility. Transmittance measurements were performed on these films. The spectra were shown in Figure 4-7.

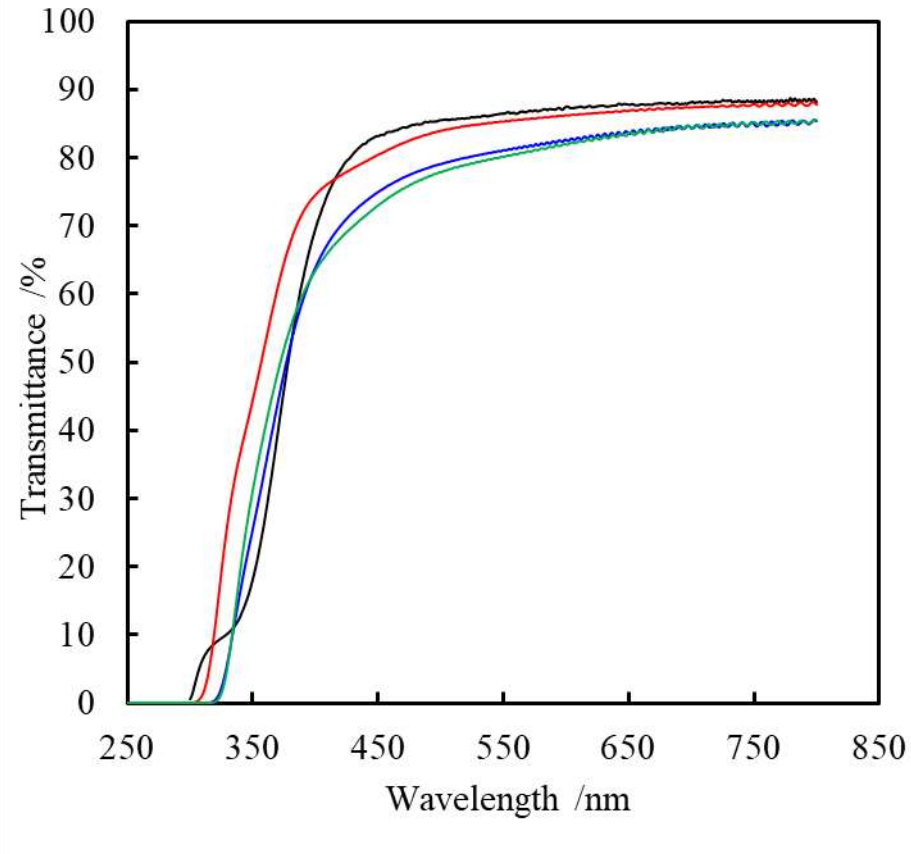

Figure 4-7. Transmittance spectra of TiO_2/WSPA-K composite films.

As shown in the figure 4-6, the films exhibited light transmittance, although visible light transmittance was reduced.

Moreover, TGA measurements were performed (Figure 4-8). The degradation temperature of the composite films were shown lower than matrix polyamide. This may be attributed to the accelerated decomposition of polyamide by the thermally excited titanium dioxide. On the other hand, ash content increased with the percentage of titanium dioxide.

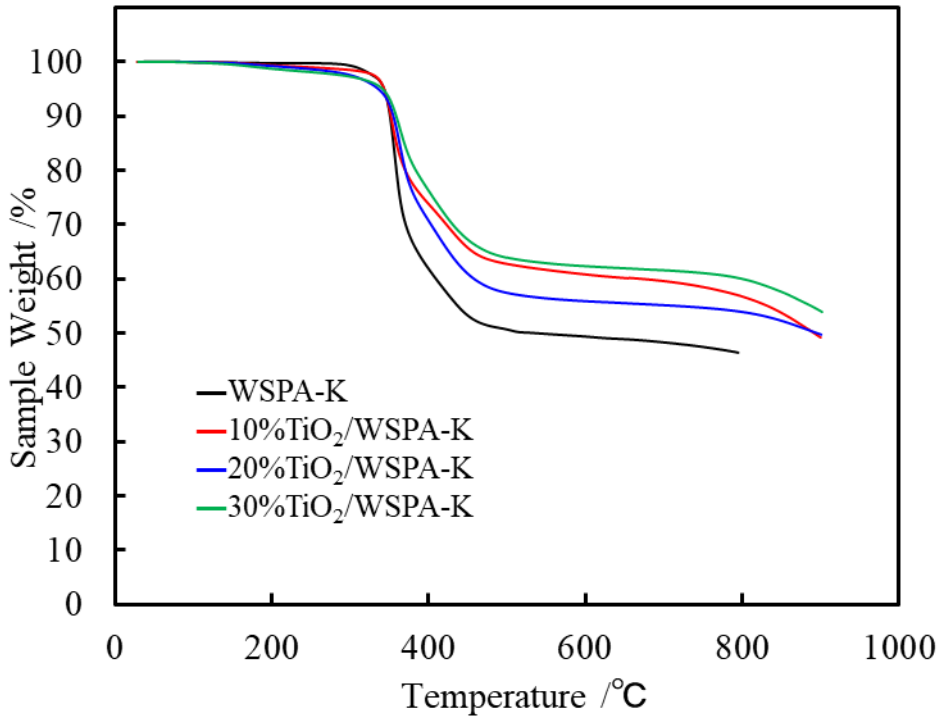

Figure 4-8. TGA curves of TiO_2/WSPA-K composite films.

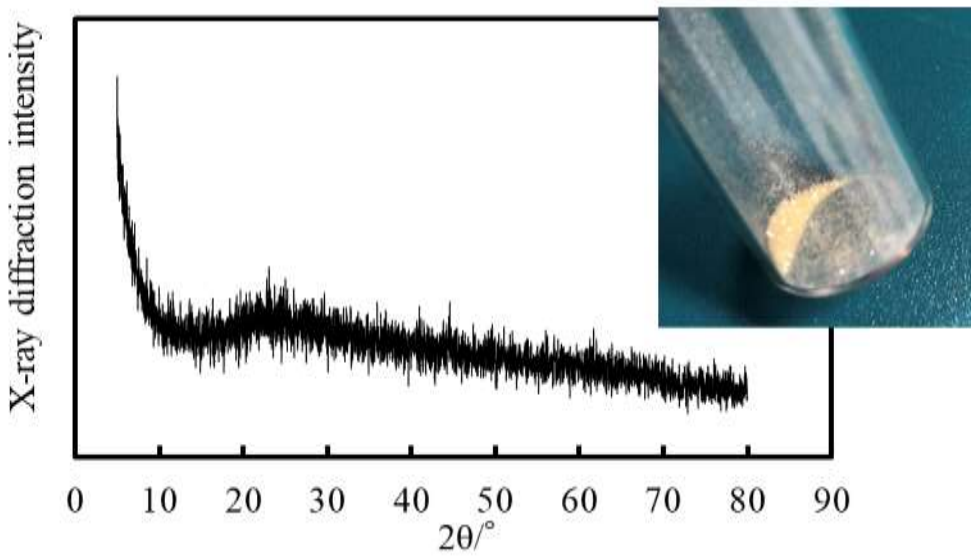

Figure 4-9. XRD pattern of 20%TiO_2/WSPA-K.

20% composite film powder XRD measurements were performed to determine the state of dispersed titanium dioxide (Figure 4-9). No sharp peaks originating from titanium

dioxide crystals were identified in the XRD pattern. This result suggests that the titanium dioxide in the composite is amorphous.

FT-IR spectra of TiO_2/WSPA-K composite films were shown in Figure 4-10. The spectra did not show any peaks from the raw material.

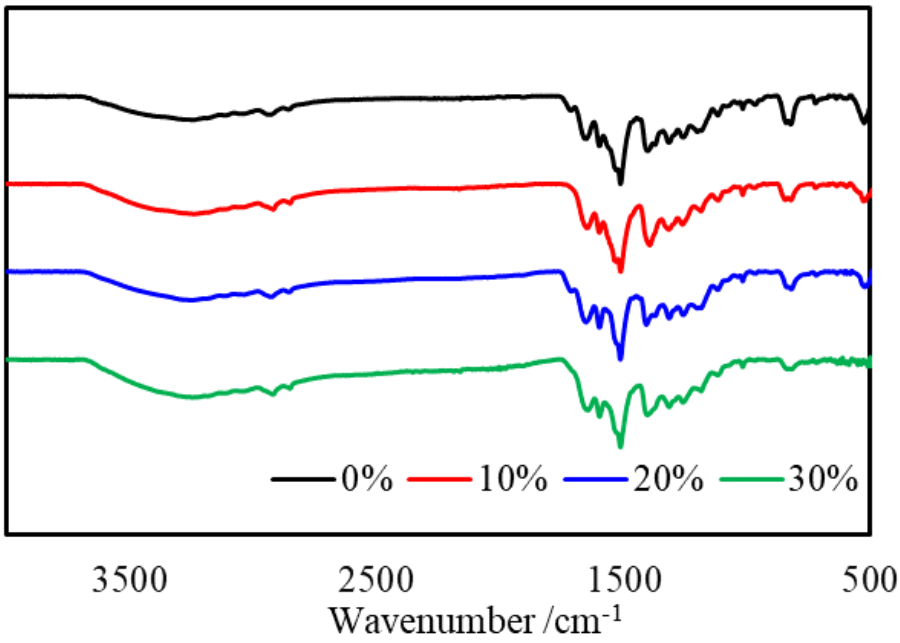

Figure 4-10. FT-IR spectra of TiO_2/WSPA-K composite films.

In addition, XPS measurements were performed to determine the state of the titanium and oxygen atoms in the composite films. The spectra were shown in Figure 4-11.

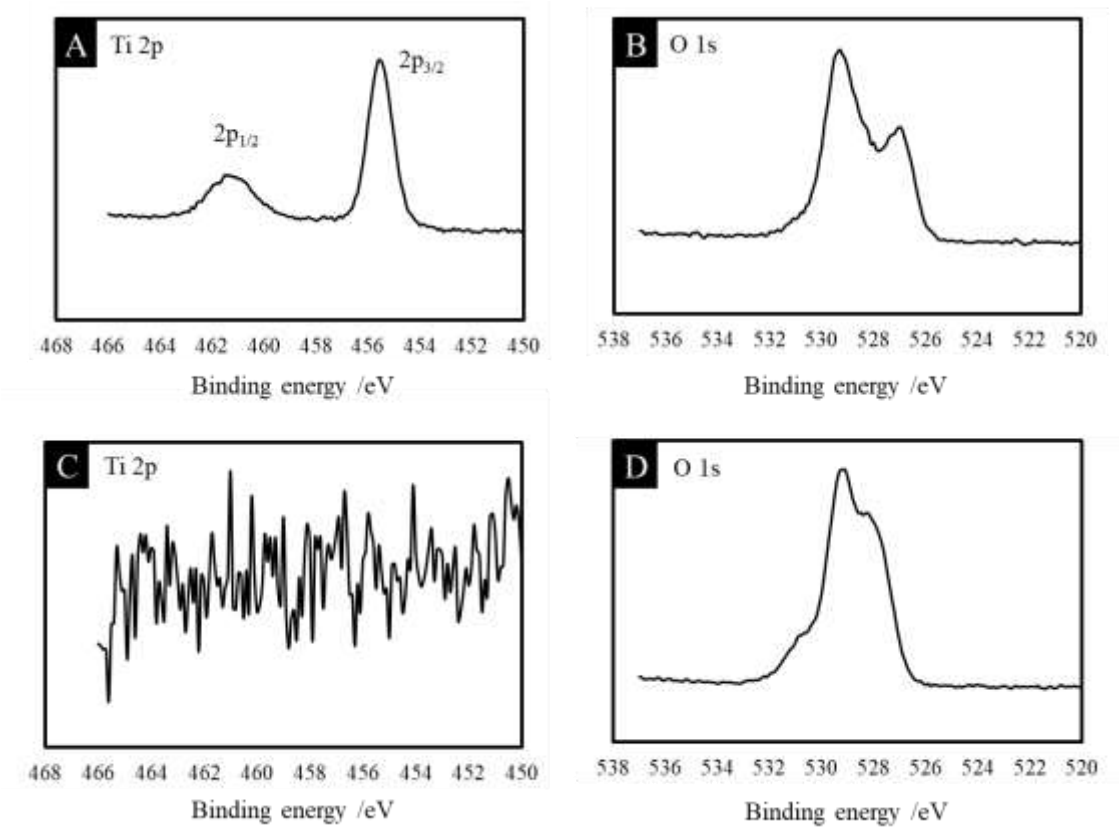

Figure 4-11. XPS spectra of 20% TiO_2/WSPA-K composite films.

A, B: XPS spectra of composite film. C, D: XPS spectra of matrix film.

The position and shape of the peaks suggested that bonds between titanium and oxygen were formed in the composite. These results indicate that amorphous titanium dioxide is present in the composite.

Finally, a TEM image of the composite film (TiO_2 ratio:30%) are shown in Figure 4-12.

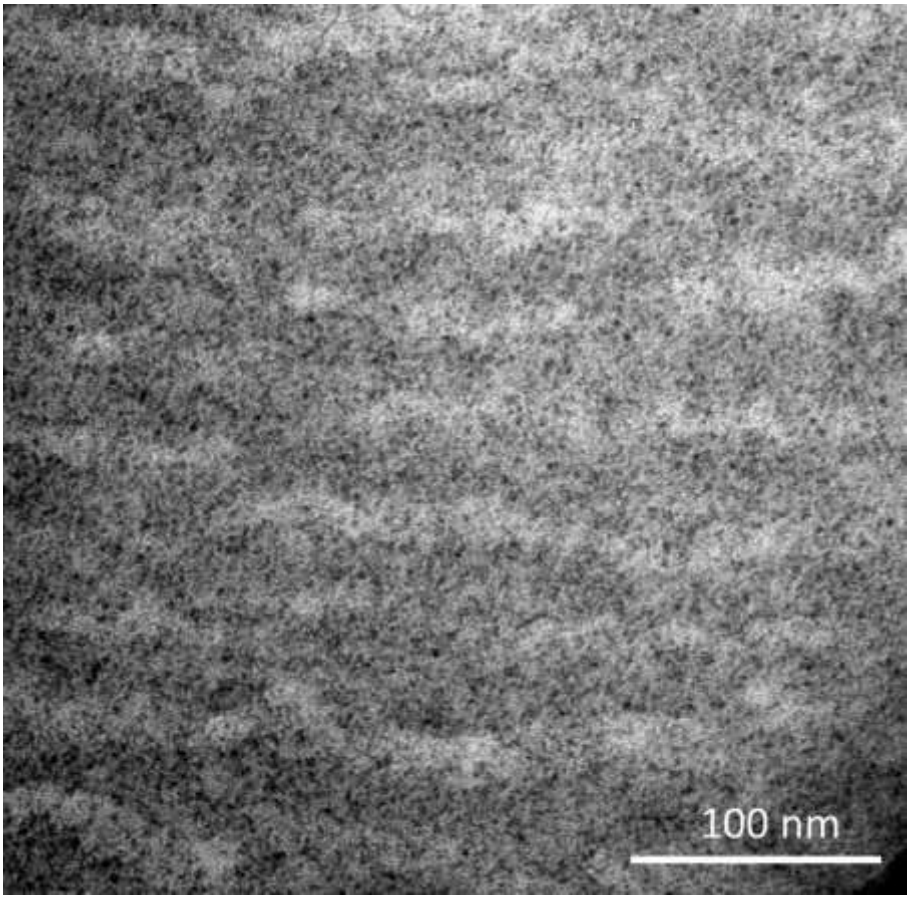

Figure 4-12. The TEM image of 30% TiO_2/WSPA-K.

In the photo, the black dots indicate the presence of TiO_2. The size of TiO_2 particles were about a few nm. In addition, the particles were uniformly dispersed in the matrix.

4.4 Conclusion

Composites of titanium dioxide and zirconium oxide with 4-aminocinnamic acid-based polyamide were prepared using a sol-gel reaction. The refractive indices of the

membranes could be controlled by the type and quantity ratio of the raw materials.

Titanium dioxide/polyamide composite films were also prepared by the same method. The films exhibited flexibility and light transmittance.

Various analyses of the films showed that the titanium dioxide particles were amorphous, a few nm in diameter, and uniformly dispersed in the matrix.

REFERENCES

1. Paquet, C.; Kumacheva, E., Nanostructured polymers for photonics, *materialstoday*, **2008**, *11*, 48-56.
2. Hasan, T.; Sun, Z.; Wang, F.; Bonaccorso, F.; Tan, P. H.; Rozhin, A. G.; Ferrari, A. C., *Adv. Mater.*, **2009**, *21*,3874–3899.
3. Persano, L.; Camposeo, A.; Pisignano, D., Active polymer nanofibers for photonics, electronics, energy generation and micromechanics, *Progress in Polymer Science*, **2015**,*43,* 48–95.
4. Edrington, A. C.; Urbas, A. M.; DeRege, P.; Chen, C. X.; Swager, T. M.; Hadjichristidis, N.; Xenidou, M.; Fetters, L. J.; Joannopoulos, J. D.; Fink, Y.; Thomas, E. L, Polymer-Based Photonic Crystals, *Adv. Mater.*, **2001**, *13*.
5. Yang, J.; Zhao, W.; Yang, Z.; He, W.; Wang, J.; Ikeda, Y.; Jiang. L., Printable photonic

polymer coating based on a monodomain blue phase liquid crystal network, *Journal of materials chemistry C*, **2019**, *44*.

6. Zhang,X.; Hosseini, A.; Polymer-Based Hybrid-Integrated Photonic Devices for Silicon On-Chip Modulation and Board-Level Optical Interconnects, *IEEE JOURNAL OF SELECTED TOPICS IN QUANTUM ELECTRONICS,* **2013**,*19*.
7. Lu, T.; Zhu, S.; Ma, J.; Lin, J.; Wang, W.; Pan, H.; Tian, F.; Zhang, W.; Zhang D.; Bioinspired Thermoresponsive Photonic Polymers with Hierarchical Structures and Their Unique Properties, *Macromol. Rapid Commun.*, **2015**, *36*, 1722−1728.
8. Othayoth, A. K.; Srinivas, B.; Murugan, K.; Muralidharan, K., Poly(methyl methacrylate)/polyphosphate blends with tunable refractive indices for optical applications, *Optical Materials*, **2020**, *104*, 1098.
9. Olshavsky, M.; Allcock, H. R., Polyphosphazenes with High Refractive Indices: Optical Dispersion and Molar Refractivity, *Macromolecules,* **1997**, *30*, 4179-4183.
10. Iino, S.; Sobu, S.; Nakabayashi, K.; Samitsu, S.; Mori, H., Highly transparent and photopatternable spirobifluorene-based
11. polythioethers with high refractive indices via thiol-ene click chemistry, *Polymer,* **2021***, 224*, 12372.
12. Chen,S.; Chen, D.; Lu, M.; Zhang,X.; Li,H.; Zhang, X.; Yang, X., Incorporating Pendent

Fullerenes with High Refractive Index Backbones: A Conjunction Effect Method for High Refractive Index Polymers, *Macromolecules*, **2015**, *48*, 8480−8488.

13. Tsai, T.; Liou, G., Highly transparent and flexible polyimide/ZrO_2 nanocomposite optical films with a tunable refractive index and Abbe number, *Chem. Commun*., **2015**, *51*, 13523-13526.

14. Lee, L.; Chen, W.; High-Refractive-Index Thin Films Prepared from Trialkoxysilane-Capped Poly(methyl methacrylate)-Titania Materials, *Chem. Mater.* , **2001**, *13*, 1137-1142.

15. Imai, Y.; Terahara, A.; Hakuta, Y.; Matsui, K.; Hayashi, H.; Ueno, N., Transparent poly(bisphenol A carbonate)-based nanocomposites with high refractive index nanoparticles, *European Polymer Journal* **2009**, *45* 630.

16. Jintoku, H.; Ihara, H., The simplest method for fabrication of high refractive index polymer–metal oxide hybrids based on a soap-free process,*Chem. Commun*., **2014**, *50*, 10611—10614.

17. Hoang, V. V.; Zung, H.; Trong, N. H. B., Structural properties of amorphous TiO2 nanoparticles, *Eur. Phys. J. D,* **2007**, *44*, 515-524.

18. Su, Y.; Cui, H.; Li, Q.; Gao, S.; Shang, J. K., Strong adsorption of phosphate by

amorphous zirconium oxide nanoparticles, *Water Research*, **2013**, *47*, 5018-5026.

Chapter 5. conclusions

4-aminocinnamic acid-based biopolyamide possess high transparency, high heat resistance, and high strength due to their unique structure. This polyamide is a polymer whose properties can be controlled by copolymerization, side-chain structure control, and compositing.

A summary of this thesis is as follows:

Chapter 2. "Self-standing Nanomembranes of Super-Tough polyamides"

Self-standing membrane even with a nanoscale thickness were developed by spin-cast of polyamides with ultra-high mechanical strength and toughness. The polyamides were designed by the polycondensation of diamine and diacid derivatives of *α*-truxillic acid, which is a photodimer of bio-based 4ACA, in the presence of aliphatic dicarboxylic acids as comonomers. In the presence of 25 mol% of pimelic acid, the synthesized polyamides possessed a mechanical strength of 470 MPa, which is the highest value reported to date for an amorphous organic material. In addition, another polyamide synthesized in the presence of 75 mol% of suberic acid was found to be super-tough with a mechanical strength of 230 MJ m^{-3}, which exceeds that of conventional fiber materials, including almost all spider webs. These exceptional mechanical properties were attributed to the orientation and tautomerization, and the conversion of non-planar cyclobutane to planar and rigid cyclobutadiene, which was stabilized under strong tension, as confirmed by *in situ*

FT-IR measurements. This conversion can induce snap-buckling like a molecular spring and enhance mechanical strength and toughness, which were higher in the synthesized polyamides as compared to those of spider silk. The nanomembrane was spin-cast to self-stand after peeling away from the glass plate.

Chapter 3 "Water-solubilization/ Insolubilization of polyamide"

4-amino cinnamic acid-based polyamide metal salts were synthesized by the action of alkali metal (Na, K and Cs) hydroxides on polyamide. The polyamides were soluble in water or methanol. The crosslinked structure was introduced by the action of alkaline earth metal (Mg, Ca, Sr and Ba) ions on this water-soluble polyamide. The polyamide was then cross-linked with alkaline earth metal ions, which gave the polyamide high chemical stability and solubility not only in water and methanol, but also in common organic solvents and strong acids. In addition, the polyamide has improved heat resistance and mechanical properties, and the barium salt in particular has greatly improved toughness.

Furthermore, composite films were prepared by dispersing cellulose nanofibers, a water-soluble filler, in the synthesized water-soluble polyamide. The resulting films, containing 1% CNF, not only had high transparency, but also showed improved mechanical properties. This is thought to be due to the interaction between the hydroxyl groups of the

cellulose nanofibers and the acetoamido group moieties of the polyamide.

These results indicate that polyamide can not only be molded and processed more safely, but also its properties can be controlled by adding metal ions and water-soluble fillers.

Chapter 4. “Compositing with nano-fillers”

Composites of titanium dioxide and zirconium oxide with 4-aminocinnamic acid-based polyamide were prepared using a sol-gel reaction. The refractive indices of the membranes could be controlled by the type and quantity ratio of the raw materials. Titanium dioxide/polyamide composite films were also prepared by the same method. The films exhibited flexibility and light transmittance.

Analyses and observations of the films showed that the titanium dioxide particles were amorphous, a few nm in diameter, and uniformly dispersed in the matrix.

It is very difficult to disperse nano-level particles, and this research case is expected to be applied not only to optical materials but also to various composite materials.

Academic achievements

Publications:

Funahashi, Y., Yoshinaka, Y., Takada, K., Kaneko, T., Self-standing Nanomembranes of Super-Tough Plastics. *Langmuir* **2021**, *38, 17*, 5128-5134.

Patent:

特願：PCT-JP2018-028270「親水性ポリアミド又はポリイミド」、発明者：金子達雄、スマントドゥイベディ、坂本茂樹、高田健司、舟橋靖芳

Conferences:

Poster presentation:

1) Yasuyoshi Funahashi, Amit Kumar, Kenji Takada, Tatsuo Kaneko, “Water-solubilization/desolbilization of high-performance biopolyamides by binding to alkali/alkaline earth metals”, Asia Pacific Society for Materials Research 2019 Annual Meeting, Sapporo, Japan, July 2019
2) Yasuyoshi Funahashi, Kenji Takada, Amit Kumar, Tatsuo Kaneko, “Water-Solubilization/Desolbilization of High-Performance Biopolyamides”, 15th IUPAC International Conference on Novel Materials and their Synthesis (NMS-ⅩⅤ), Shenynag, China, September 2019
3) Yasuyoshi Funahashi, Kenji Takada, Amit Kumar, Tatsuo Kaneko, ”Preparation

of water soluble, high-performance biopolyamides with alkaline earth/alkali metals” Japan-South-East Asia Collaboration Hub of Bioplastics Study ,Fukui, Japan, September 2019

4) 舟橋靖芳,高田健司,Kumar Amit,金子達雄, “4-アミノ桂皮酸由来水溶性バイオポリアミドの合成”, 令和元年度　エクセレントコア「天然マテリアル」研究拠点シンポジウムプログラム　第１１回サクラン研究会　年次大会, 石川, 日本, 2019 年 10 月

5) 舟橋靖芳,高田健司,Kumar Amit,金子達雄, “バイオトルキシル酸由来水溶性アラミドの網目構造制御”, 第 31 回高分子ゲル研究討論会, 東京, 日本, 2020 年 1 月

6) 舟橋靖芳,高田健司,Kumar Amit,村田英幸,金子達雄, “4-アミノ桂皮酸由来ポリアミド薄膜の作製”, 19-3 エコマテリアルシンポジウム, 東京, 日本, 2020 年 3 月

・Oral presentation

1) 舟橋靖芳,高田健司,金子達雄, “4-アミノ桂皮酸由来水溶性ポリアミドの合成と物性評価”, 第 68 回高分子年次大会, 大阪,日本, 2019 年 5 月

2) 舟橋靖芳,Kumar Amit,高田健司,金子達雄, “トルキシル酸由来の剛直バイオポリアミド塩の水溶性制御” 第 68 回高分子討論会, 福井, 日本, 2019 年 9 月

3) 舟橋靖芳,高田健司,Kumar Amit,金子達雄, “4-アミノ桂皮酸由来バイオポリアミ

ドの合成と水溶性制御” 第 8 回日本バイオマテリアル学会　北信越ブロック若手研究発表会, 石川, 日本, 2019 年 12 月

4) Yasuyoshi Funahashi, Kenji Takada, Amit Kumar, Tatsuo Kaneko, Preparation of 4-aminocinnamic acid based polyamides and their self-standing nano-films, Pacifichem 2021, 2021 年 12 月 16-21 日

5) 舟橋靖芳、吉中陽平、高田健司、金子達雄、「4-アミノ桂皮酸由来バイオポリアミド共重合体の合成および高力学物性ファイバーと薄膜の作製」、第 71 回高分子討論会、2022 年 9 月

Award:

Best poster award, Japan-South-East Asia Collaboration Hub of Bioplastics Study, September 2019